Supporting Information for:

Assessing inter- and intramolecular continuous-flow strategies towards methylphenidate (Ritalin) hydrochloride

Romaric Gérardy,[a] Marc Winter,[b] Alessandra Vizza,[b] Jean-Christophe M. Monbaliu[a,*]

[a] *Center for Integrated Technology and Organic Synthesis, Department of Chemistry, University of Liège, B-4000 Liège (Sart Tilman), Belgium*
[b] *Corning Reactor Technologies, Corning SAS, 7 bis, Avenue de Valvins CS 70156 Samois sur Seine, 77215 Avon Cedex - France*

E-mail: jc.monbaliu@ulg.ac.be

Table of contents

1 Continuous-flow setups

1.1 Generalities

1.1.1 Pumps

Chemyx Nexus 3000 and Nexus 6000 syringe pumps were used to handle the feed solutions of tetrabutylammonium azide (nBu$_4$NN$_3$), tosyl chloride (TsCl), *p*-toluenesulfonyl azide (TsN$_3$), methyl phenylacetate (**2a**) and 1,8-diazabicyclo[5.4.0]undec-7-ene (DBU) in NMP, methyl phenyldiazoacetate (**4a**), *N*-Boc piperidine (**3a**) and Rhodium(II) octanoate dimer (Rh$_2$(oct)$_4$) in hexane, 4-methyl-*N*'-(2-oxo-1-phenyl-2-(piperidin-1-yl)ethylidene)benzene sulfono-hydrazide (**3b**), DBU and Aliquat® 336 in toluene and HCl in ether/methanol or dioxane/methanol. The feed solutions were loaded in Chemyx® stainless steel 5 or 20 mL syringes equipped with Dupont™ Kalrez® Spectrum™ AS-568 o-rings (0.239 x 0.070" or 0.549 x 0.103").

ThalesNano® micro HPLC pumps (0.01 – 10 mL min^{-1}, max 80 bar, wetted parts: SS 316, ruby and sapphire) were utilized to inject the extraction solvents (10 wt% and 15 wt% aqueous sodium chloride and hexane) and the feed solutions of 4-methyl-*N*'-(2-oxo-1-phenyl-2-(piperidin-1-yl)ethylidene)benzene sulfonohydrazide (**3b**), DBU and Aliquat® 336 in toluene for the mesoscale experiments (Corning® Advanced-Flow™ Low-Flow reactor).

A FUJI Technologies™ pump (triplex plunger pump HYM-08) was utilized to handle the feed solutions of 4-methyl-*N*'-(2-oxo-1-phenyl-2-(piperidin-1-yl)ethylidene)benzene sulfonohydrazide (**3b**), DBU and Aliquat® 336 in toluene for the mesoscale experiments (Corning® Advanced-Flow™ G1 reactor).

1.1.2 Microfluidic reactor elements

1.1.2.1 PFA loops and packed-bed reactors

The microfluidic reactors were constructed with high purity PFA coils (high purity DuPont® PFA tubing, 1/16" o.d., 1/32" i.d.) of various internal volumes (0.5, 1.0, 1.5, 2 and 6 mL internal volume).

Packed bed reactors were constructed with 1/4" PFA tubing, Swagelok® connectors (1/16" o.d. tubing), stainless steel Swagelok® tube fittings, stainless steel Swagelok® reducing unions (1/4 " x 1/16" o.d. tubing) and stainless steel Swagelok® connectors (for 1/4" o.d. tubing). If specified, they were heated in a Jones Chromatography® 7971 column heater. Glass beads (0.1 mm diameter, Sigma-Aldrich) were used as packing material.

1.1.2.2 Connectors, ferules and mixers

Fluidic connectors were purchased from IDEX/Upchurch: Upchurch Scientific® Super Flangeless™ nuts (natural PEEK, 1/4-28 thread for 1/16" o.d. tubing), Upchurch Scientific® Super Flangeless™ ferrules (yellow ETFE w/SST Ring for 1/16" o.d. tubing), Upchurch Scientific® T-mixers (natural PEEK 1/4-28 thread for 1/16" o.d. tubing, 0.02" through hole),

Upchurch Scientific® cross junctions (natural PEEK 1/4-28 thread for 1/16” o.d. tubing, 0.02” through hole) and Upchurch Scientific® unions (ETFE, 1/4-28 thread for 1/16”).

1.1.2.3 Extraction and liquid-liquid separation module

The extraction and liquid-liquid separation module usually consisted of a cross junction (Upchurch Scientific®, natural PEEK 1/4-28 thread for 1/16” o.d. tubing, 0.02” through hole) for the concomitant injection of hexane and aqueous sodium chloride (15 wt%), a short packed-bed column (packing material: 0.1 mm glass beads) and a continuous-flow liquid-liquid membrane separator (Zaiput Flow Technologies®) with a PTFE membrane (0.5 µm pores). Dome-type back-pressure regulators were inserted on the permeate and retentate outlets, and set at appropriate cracking pressures to ensure smooth and efficient phase separation. The aqueous outlet was connected to a waste tank, and the organic outlet was connected to a collection vial, or connected to the next microfluidic reactor.

In some examples, the extraction and liquid-liquid separation module consisted of a T-mixer (Upchurch Scientific®, natural PEEK 1/4-28 thread for 1/16" o.d. tubing, 0.02” through hole for the injection of aqueous sodium chloride (10 wt%), a short packed-bed column (packing material: 0.1 mm glass beads) and a continuous-flow liquid-liquid membrane separator (Zaiput Flow Technologies®) with a PTFE membrane (0.5 µm pores). Dome-type back-pressure regulators were inserted on the permeate and retentate outlets and set at appropriate cracking pressures to ensure smooth and efficient phase separation. The aqueous outlet was connected to a waste tank, and the organic outlet was connected to a collection vial, or connected to the next microfluidic reactor.

1.1.2.4 Back-pressure regulator

Dome-type back-pressure regulators (BPRs) were used (Zaiput Flow Technologies®). These BPRs were connected to a compressed gas cylinder (air or nitrogen) to set the pressure. In some examples where accurate pressure control was not mandatory, standard HPLC-type BPRs (IDEX/Upchurch Scientific, 75 or 250 psi) or manually adjustable spring-type BPRs (FutureChemistry®) were utilized.

1.1.3 Continuous-flow photoreactor

The microscale photoreactor (Figure S1) was machined at the Central Machine Shop of the Faculty of Sciences with 24 LED Engin® high efficiency violet LED emitters (395 nm, 1150 mW @ IF = 700 mA, Viewing Angle $2\theta_{1/2}$ = 68°, Total Included Angle $\theta_{0.9V}$ = 100°). The LED emitters were alimented with two Tenma® DC power supply 72-8695A (0-32V, 0-3 A). The microscale photoreactor consisted in a docking station with eight guide rails arranged symmetrically around a central hub. The central hub comprised a microreactor made of 1/16" PFA coil (2 mL internal volume, 800 µm internal diameter, cf. Figures S1&S10) wrapped around a thermoregulated cylinder. Each guide rail hosted an adjustable heat sink

pillar which supported three high power LEDs mounted to face towards the PFA coil reactor. The 8 heat-sink integrated pillars were sized to remove the heat produced by the LEDs.

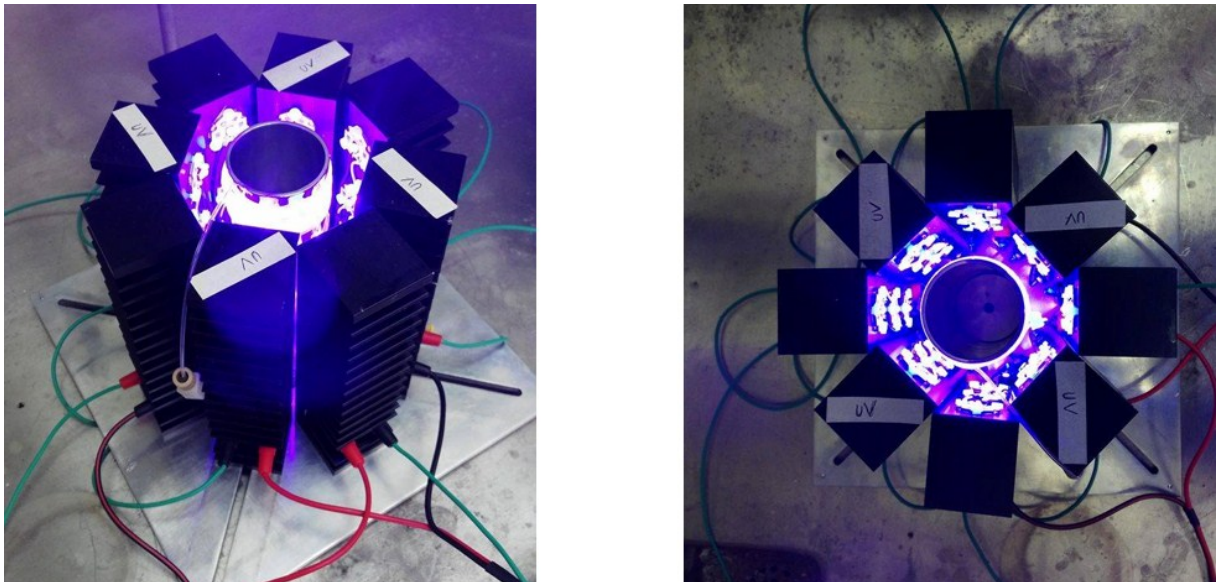

Figure S1. Microscale continuous-flow photoreactor

1.1.4 Mesofluidic reactors

Corning® Advanced-Flow™ reactors were utilized for mesoscale experiments. Corning® Advanced-Flow™ reactors are specially designed for the seamless transition from lab feasibility to process development to industrial-scale production of chemicals. The Low-Flow and the G1 reactors are the most versatile of the lab scale reactors, mainly used for process development and optimization of chemical reactions.

Corning® Advanced-Flow™ reactors were manufactured and engineered by Corning S.A.S with several glass fluidic modules connected in series. Each fluidic module was designed with a specific number of inlets and integrated by two layers of heat exchanger. The configuration of the Corning® Advanced-Flow™ Low-Flow reactor involved 4 fluidic modules of 0.5 mL internal volume each connected in series (Figure S2). The configuration of the Corning® Advanced-Flow™ G1 reactor involved 4 fluidic modules (FMs) of 9 mL internal volume each connected in series for the thermolysis, and one additional fluidic module for cooling the reactor effluent (T = 10 °C) before the BPR (Figure S3). For safety reasons, the reactors were installed in a closed fume hood and were operated at 180 °C and 5 bar.

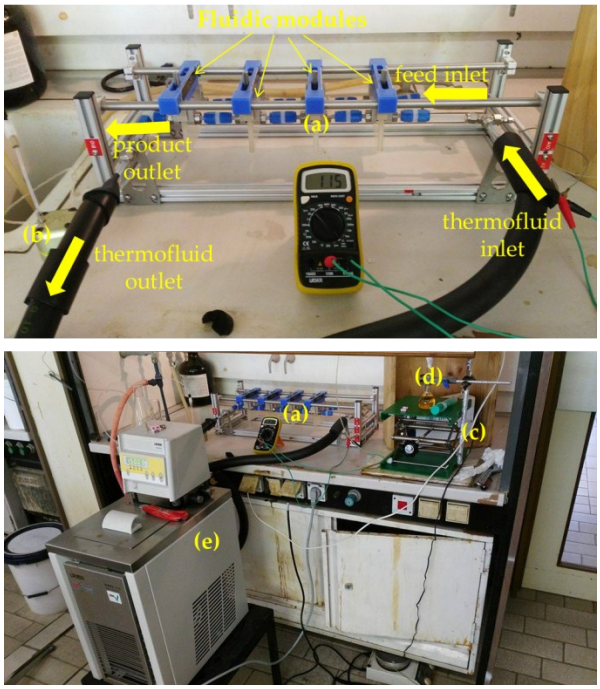

Figure S2. Corning® Advanced-Flow™ Low-Flow setup. (a): reactor configuration showing the 4 fluidic modules, (b): BPR, (c) HPLC pump, (d): feed solution, (e) thermostat

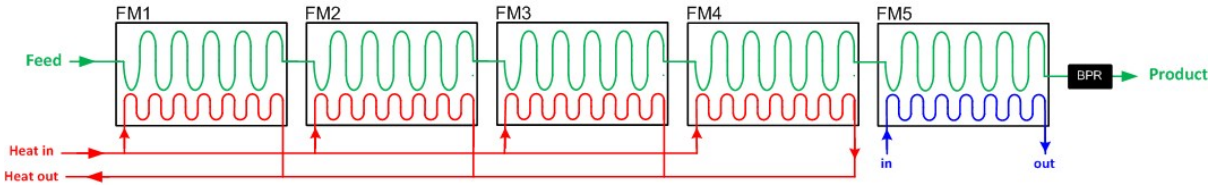

Figure S3. Configuration of the Corning® Advanced-Flow™ G1 reactor showing the 4 fluidic modules (FMs) operated at 180 °C (red) and the FM operated at 10 °C (blue) before the BPR

1.1.5 Thermoregulatory devices

PFA microreactor coils were maintained in thermoregulated oil baths (MR Hei-Tec equipped with a Pt-1000 thermocouple). LAUDA® Proline RP 845 thermostat or LAUDA® Integral XT750 (silicone oil Kryo 20) were used for the thermoregulation of the mesofluidic reactors (Corning® Advanced-Flow™ Low-Flow reactor and Corning® Advanced-Flow™ G1 reactor).

1.2 Detailed microfluidic setups

The reader is referred to the main manuscript for experimental details (Feed concentrations, flow rates, counter-pressures).

1.2.1 Continuous-flow preparation of tosyl azide (TsN_3)

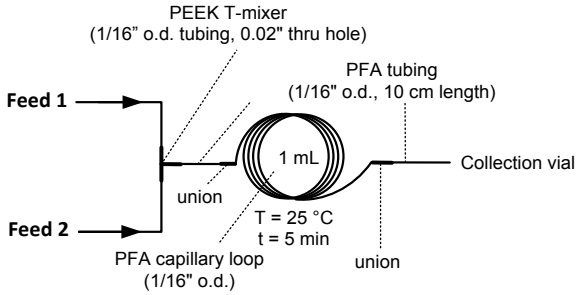

Figure S4. Detailed microfluidic setup for the continuous-flow preparation of tosyl azide

1.2.2 Continuous-flow preparation and purification of methyl phenyldiazoacetate (**4a**)

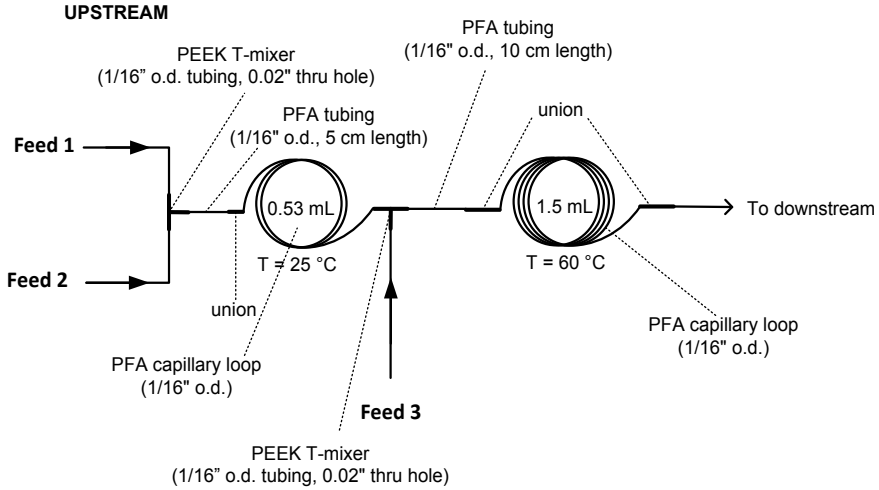

Figure S5. Detailed microfluidic setup for the continuous-flow preparation of methyl phenyldiazoacetate (upstream)

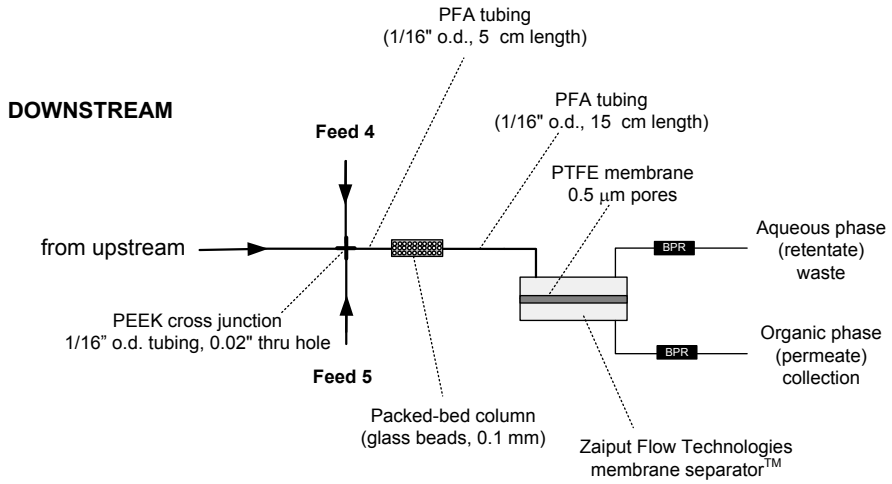

Figure S6. Detailed microfluidic setup for the continuous-flow preparation of methyl phenyldiazoacetate (downstream)

1.2.3 Continuous-flow C-H carbene insertion towards *N*-Boc methylphenidate (**5a**)

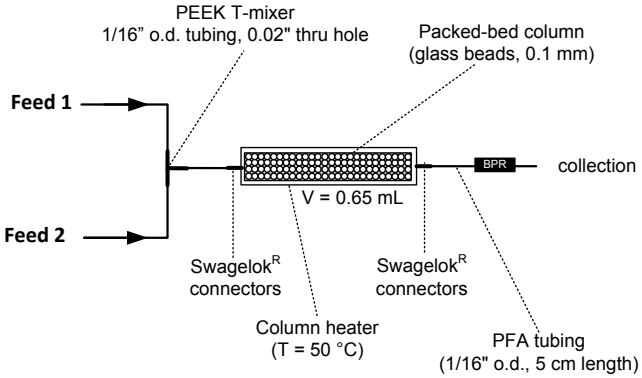

Figure S7. Detailed microfluidic setup for the continuous-flow C-H carbene insertion towards *N*-Boc methylphenidate

1.2.4 Telescoped continuous-flow preparation of *N*-Boc methylphenidate (**5a**)

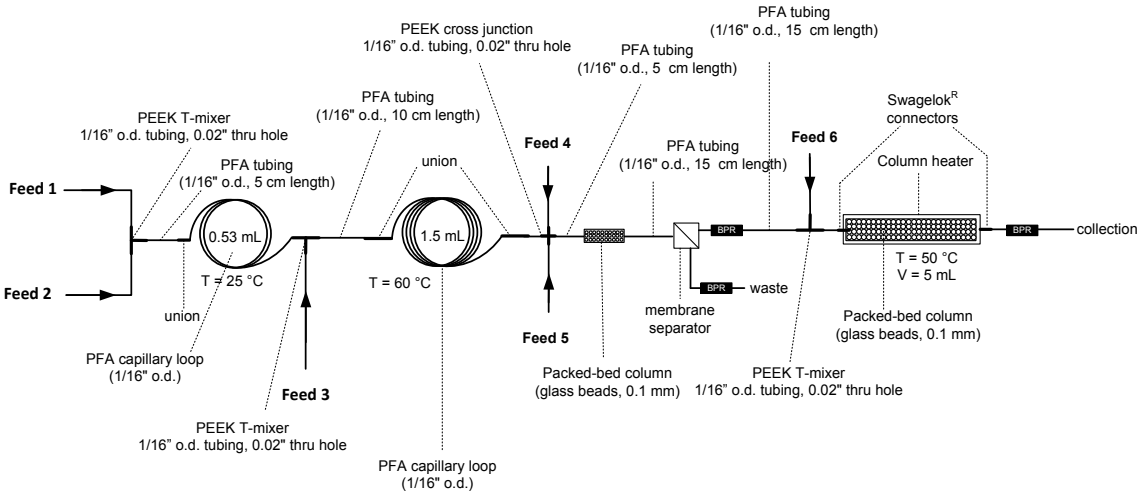

Figure S8. Detailed microfluidic setup for the telescoped continuous-flow intermolecular preparation of *N*-Boc methylphenidate

1.2.5 Continuous-flow thermolysis of tosylhydrazone **3b** towards β-lactam **5b**

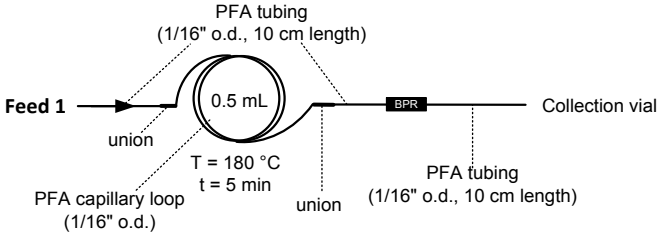

Figure S9. Detailed microfluidic setup for the continuous-flow thermolysis of tosylhydrazone **3b**

1.2.6 Continuous-flow photolysis of tosylhydrazone **3b** towards β-lactam **5b**

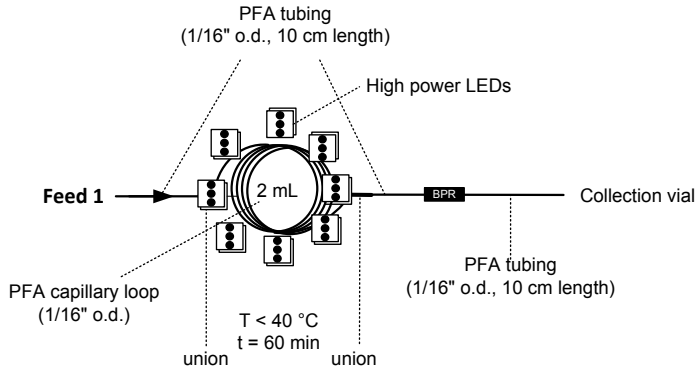

Figure S10. Detailed microfluidic setup for the continuous-flow photolysis of tosylhydrazone **3b**

1.2.7 Fully telescoped continuous-flow intramolecular preparation of methylphenidate hydrochloride (**1**·HCl)

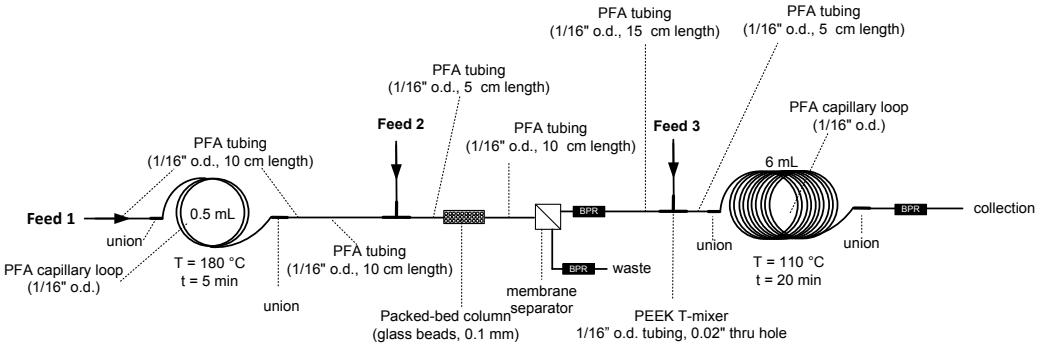

Figure S11. Detailed microfluidic setup for the fully telescoped continuous-flow intramolecular preparation of methylphenidate hydrochloride

2 Supplemental experimental data

2.1 Generalities

^{1}H NMR spectra were recorded at 250 or 400 MHz and ^{13}C NMR spectra were recorded at 62.8 MHz or 100.6 MHz on Bruker Avance spectrometers. The chemical shifts are reported in ppm relative to TMS as internal standard or to solvent residual peak. HPLC analyses were performed on a Waters setup (Alliance 2695 system, Empower software) with a 996 PDA UV detector (190–400 nm) using a X-Terra® RP18 column (150 x 4.6 mm, 3.5 µm). Chiral HPLC experiments were performed on a Waters 600 (Empower software) with a 996 PDA UV detector using a Daicel® Chiralpak AD column (250 x 4.6 mm, 10 µm). GC-MS analyses were performed on a Thermo® Scientific ThermoQuest TraceGC setup equipped with a Varian® FactorFour VF-5MS (40 m x 0.20 mm, 0.33 µm) column and with a Thermo® PolarisQ Finnigan mass spectrometer. IR spectra were recorded using ATR technique on a Thermo® Scientific Nicolet™ IS™ 5 FT-IR spectrometer. Melting points were determined with a Stuart Scientific® Melting Point Apparatus SMP3 (uncorrected values). HRMS spectra were recorded on a FTMS (ESI) apparatus (Thermo® Scientific Q Exactive™). Solvents were purchased from Labotec, and anhydrous dichloromethane and hexane were obtained by distillation over CaH_2. Commercially available chemicals (Sigma-Aldrich or TCI) were used as received, unless otherwise noted. The average molecular weight of Aliquat® 336 was 442 g mol^{-1}. Moisture sensitive reactions were conducted under an argon atmosphere. Column chromatography was performed using Davisil® LC60A 70-200 µm silica gel while TLC was conducted on Merck® F254 silica gel precoated plates. Kugelrohr distillations were performed on a Büchi® glass oven B-585.

2.2 Additional experimental procedures

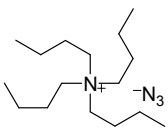

$C_{16}H_{36}N_4$
Mol. Wt.: 284.48

Tetrabutylammonium azide.[S1] 12 g (0.185 mol, 2 eq.) of sodium azide in 14 mL of water were added to 60 g of a 40% tetrabutylammonium hydroxide aqueous solution (92.5 mmol, 1 eq.). The mixture was vigorously stirred in a separatory funnel and extracted with ethyl acetate (1 x 75 mL, then 3 x 20 mL). The combined organic fractions were dried over sodium sulfate, filtered and concentrated under vacuum to give a thick yellow oil, that crystallized as a white solid (21.2 g, 80%), when placed several days under vacuum over P_2O_5. **^{1}H NMR ($CDCl_3$, 400 MHz):** δ = 3.23-3.47 (m, 8H), 1.70 (dt, *J* = 15.7, 7.9 Hz, 8H), 1.47 (dq, *J* = 14.4, 7.2 Hz, 8H), 1.02 (t, *J* = 7.2 Hz, 12H) ppm.

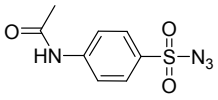

$C_8H_8N_4O_3S$
Mol. Wt.: 240.24

***p*-Acetamidobenzenesulfonyl azide**.[S2] *p*-Acetamidobenzenesulfonyl chloride (1.04 g, 4.33 mmol, 1 eq.) and acetone (40 mL) were stirred in a round-bottom flask cooled in an ice bath for 15 minutes. Then, sodium azide (0.29 g, 4.46 mmol, 1 eq.) was added, and the mixture was allowed

to evolve to room temperature under stirring for 48 h. Next, acetone was removed under reduced pressure and the resulting crude material was dissolved in 120 mL of ethyl acetate. The solution was washed with 50 mL of brine, dried over sodium sulfate, filtered and the solvent was removed under vacuum. This yielded 1 g (96%) of *p*-ABSA as a yellow-white solid. **^{1}H NMR ($CDCl_3$, 400 MHz):** δ = 7.89 (d, *J* = 8.9 Hz, 2H), 7.78 (d, *J* = 8.9 Hz, 2H), 2.25 (s, 3H) ppm; **^{13}C NMR ($CDCl_3$, 100.6 MHz):** δ = 168.9, 143.9, 132.6, 129.0, 119.5, 24.8 ppm. The NMR data matched those reported in the literature.[S3] **ESI HRMS** *m/z* $C_8H_9N_4O_3S^+$ $[M+H]^+$: calcd 241.0390. Found: 241.0390.

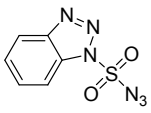

$C_6H_4N_6O_2S$
Mol. Wt.: 224.2

Benzotriazol-1-yl-sulfonyl azide.[S4] Sulfuryl chloride (6.23 mL, 0.08 mol, 1 eq.) was added dropwise to a suspension of sodium azide (5 g, 0.08 mol, 1 eq.) in acetonitrile (25 mL) at 0 °C, and the resulting suspension was stirred overnight at room temperature. Benzotriazole (18.35 g, 0.15 mol, 1.9 eq.) was dissolved in pyridine (6.46 mL, 0.08 mol, 1 eq.) and acetonitrile (10 mL), and the resulting solution was added dropwise to the suspension containing chlorosulfonylazide at 0 °C. The resulting mixture was stirred for 10 h at room temperature. The white precipitate was removed by filtration. The orange filtrate was diluted with water (100 mL) and extracted with ethyl acetate (3 x 50 mL). The combined organic phase was next washed with aqueous Na_2CO_3 (10% wt, 2 x 50 mL), brine (1 x 50 mL) and dried over Na_2SO_4. Half the amount of ethyl acetate was removed under reduced pressure (water bath temperature < 30 °C). Hexane (100 mL) was added, and the remaining solution was left at 4 °C overnight. Benzotriazol-1-yl-sulfonyl azide was collected upon filtration as an off-white solid (12.1 g, 67%).**^{1}H NMR ($CDCl_3$, 400 MHz):** δ = 8.20 (d, *J* = 8.3 Hz, 1H), 7.94 (d, *J* = 8.4 Hz, 1H), 7.74 (t, *J* = 7.8 Hz, 1H), 7.59 (t, *J* = 7.7 Hz, 1H) ppm. **^{13}C NMR ($CDCl_3$, 100.6 MHz):** δ = 145.0, 131.2, 126.6, 121.0, 111.8 ppm. The NMR data matched those reported in the literature.[S4] **ESI HRMS** *m/z* $C_6H_5N_6O_2S^+$ $[M+H]^+$: calcd 225.0189. Found: 225.0190.

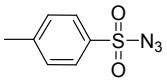

$C_7H_7N_3O_2S$
Mol. Wt.: 197.21

***p*-Toluenesulfonyl azide**.[S5] Tosyl chloride was recrystallized using a literature procedure.[S6] Tosyl chloride (1.5 g, 7.87 mmol, 1 eq.) was dissolved in H_2O/acetone 1:1 (40 mL) in a round-bottom flask cooled in an ice bath, and stirred for 15 minutes. Then, sodium azide (0.75 g, 11.54 mmol, 1.5 eq.) was added, and the mixture was allowed to evolve to room temperature under stirring for 24 h. Next, acetone was removed under vacuum, and the resulting mixture was extracted with 3 x 20 mL of ethyl acetate. The combined organic fractions were washed with 20 mL of brine, dried over sodium sulfate, filtered and the solvent was removed under reduced pressure. This yielded 1.35 g (87%) of tosyl azide as a transparent oil that crystallized upon standing in a fridge. **^{1}H NMR ($CDCl_3$, 400 MHz):** δ = 7.84 (d, *J* = 8.4 Hz, 2H), 7.41 (d, *J* = 8.1 Hz, 2H), 2.48 (s, 3H) ppm. **^{13}C NMR ($CDCl_3$, 100.6 MHz):** δ = 146.3, 135.6, 130.4, 127.6, 21.9 ppm. The NMR data matched those reported in the literature.[S5] **ESI HRMS** *m/z* $C_7H_7N_3NaO_2S^+$ $[M+Na]^+$ calcd: 220.0151. Found: 220.0152.

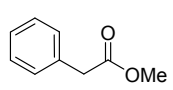

$C_9H_{10}O_2$
Mol. Wt.: 150.17

Methyl phenylacetate (2a).[S7] Phenylacetic acid (10 g, 73.45 mmol) was dissolved in 100 mL of methanol in the presence of concentrated H_2SO_4 (6 drops). The mixture was heated to 70 °C under stirring for 6 h. Methanol was removed under reduced pressure, and the crude material was dissolved in 50 mL of ethyl acetate. It was then washed with 5 x 25 mL of aqueous Na_2CO_3 (10 wt%), dried over sodium sulfate and filtered. Ethyl acetate was removed under vacuum to give 11 g (quant.) of methyl phenylacetate (**2a**) as a transparent oil. **^{1}H NMR ($CDCl_3$, 400 MHz):** δ = 7.21-7.35 (m, 5H), 3.67 (s, 3H), 3.62 (s, 2H) ppm. **^{13}C NMR ($CDCl_3$, 100.6 MHz):** δ = 171.9, 133.9, 129.2, 128.5, 127.0, 51.9, 41.1 ppm. The NMR data matched those reported in the literature.[S8] **ESI HRMS** *m/z* $C_9H_{11}O_2^+$ $[M+H]^+$: calcd 151.0754. Found: 151.0754.

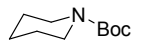

$C_{10}H_{19}NO_2$
Mol. Wt.: 185.26

***N*-Boc-piperidine (3a)**.[S9] Piperidine was distilled prior to use. Piperidine (6.6 mL, 66 mmol, 1.1 eq.) and di-*tert*-butyl dicarbonate (13.1 g, 60 mmol, 1 eq.) were stirred in dichloromethane (200 mL) for 4 h at room temperature. Dichloromethane was removed under reduced pressure, and the resulting crude material was purified by Kugelrohr distillation to give 9.3 g (80%) of *N*-Boc-piperidine (**3a**) as a transparent oil. **^{1}H NMR ($CDCl_3$, 400 MHz):** δ = 3.32-3.39 (m, 4H), 1.48-1.62 (m, 6H), 1.46 (s, 9H) ppm. **^{13}C NMR ($CDCl_3$, 100.6 MHz):** δ = 155.1, 79.2, 28.6, 25.9, 24.6 ppm. The NMR data matched those reported in the literature.[S9] **ESI HRMS** *m/z* $C_{10}H_{19}NNaO_2^+$ $[M+Na]^+$: calcd 208.1308. Found: 208.1307.

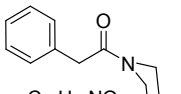

$C_{13}H_{17}NO$
Mol. Wt.: 203.28

2-Phenyl-1-(piperidin-1-yl)ethanone.[S10] To a solution of phenylacetyl chloride (20 mL, 0.15 mol, 1 eq.) in dichloromethane (200 mL) was added dropwise piperidine (37.54 mL, 0.38 mol, 2.5 eq.) at 0 °C under vigorous stirring. After complete addition, the reaction mixture was stirred overnight at room temperature. The reaction was quenched by adding aqueous HCl (1 M, 50 mL). The organic phase was washed with aqueous $NaHCO_3$ (10 wt%, 3 x 50 mL), brine (1 x 50 mL), dried over Na_2SO_4, filtered and concentrated under vacuum. The yellow oil was then distilled under reduced pressure (0.02 bar, 150 °C) to yield 2-phenyl-1-(piperidin-1-yl)ethanone as an uncoloured oil (86%, 25.9 g). **^{1}H NMR ($CDCl_3$, 400 MHz):** δ = 7.28-7.34 (m, 2H), 7.20-7.27 (m, 3H), 3.73 (s, 2H), 3.53-3.60 (m, 2H), 3.33-3.40 (m, 2H), 1.48-1.62 (m, 4H), 1.30-1.36 (m, 2H) ppm. **^{13}C NMR ($CDCl_3$, 100.6 MHz):** δ = 169.1, 135.4, 128.6, 128.5, 126.6, 47.2, 42.8, 41.1, 26.1, 25.4, 24.4 ppm. The NMR data matched those reported in the literature.[S10] **ESI HRMS** m/z $C_{13}H_{18}NO^+$ $[M+H]^+$**:** calcd 204.1383. Found: 204.1385.

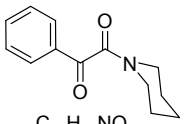

$C_{13}H_{15}NO_2$
Mol. Wt.: 217.26

1-Phenyl-2-(piperidin-1-yl)ethane-1,2-dione.[S11] 86.6 mL (0.61 mol, 1 eq.) of methyl benzoylformate (**2b**) and 60.4 mL (0.61 mol, 1 eq.) of piperidine were stirred at 105 °C for 4 h. The reaction mixture was then cooled to room temperature, triturated in petroleum spirit 40-60 and filtered to give 113.6 g (86%) of 1-phenyl-2-(piperidin-1-yl)ethane-1,2-dione as a white solid. **^{1}H NMR ($CDCl_3$, 400 MHz):** δ = 7.92-7.98 (m, 2H), 7.61-7.67 (m, 1H), 7.51 (t, *J* = 7.7 Hz, 2H), 3.66-3.75 (m, 2H), 3.25-3.33 (m, 2H), 1.66-1.74 (m, 4H), 1.52-1.56 (m, 2H) ppm. **^{13}C NMR ($CDCl_3$, 100.6 MHz):** δ = 191.9, 165.4, 134.6, 133.2, 129.5, 129.0, 47.0, 42.1, 26.1, 25.4, 24.3 ppm. The NMR data matched those reported in the literature.[S12] **ESI HRMS** *m/z* $C_{13}H_{16}NO_2^+$ $[M+H]^+$: calcd 218.1176. Found: 218.1178. MP**:** 104.7-106.3 °C (literature:[S12] 104-106 °C).

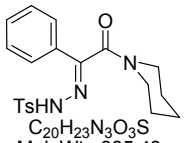

$C_{20}H_{23}N_3O_3S$
Mol. Wt.: 385.48

4-Methyl-N'-(2-oxo-1-phenyl-2-(piperidin-1-yl)ethylidene)benzenesulfono hydrazide (3b).[S11] 54.3 g (0.25 mol, 1 eq.) of 1-phenyl-2-(piperidin-1-yl)ethane-1,2-dione, 50.1 g (0.27 mol, 1.1 eq.) of *p*-toluenesulfonyl hydrazide and 3 g (0.016 mol, 0.06 eq.) of *p*-toluenesulfonic acid monohydrate were stirred in MeCN (600 mL) for 15 h at 90 °C. MeCN was then removed under reduced pressure, and could be recycled for other batches. The resulting white solid was washed with diethyl ether and recrystallized from boiling ethanol. After filtration, the white needles were washed with diethyl ether to give 81.2 g (84%) of pure tosylhydrazone **3b.** The mother liquor was distilled and ethanol could be recycled for other recrystallizations. **^{1}H NMR (DMSO-d_6, 400 MHz):** δ = 11.25 (s, 1H), 7.82 (d, *J* = 8.3 Hz, 2H), 7.47- 7.51 (m, 2H), 7.40-7.46 (m, 5H), 3.58 (brs, 2H), 3.00 (t, *J* = 5.5 Hz, 2H), 2.37 (s, 3H), 1.57 (brs, 4H), 1.30 (brs, 2H) ppm. **^{13}C NMR (DMSO-d_6, 100.6 MHz):** δ = 161.5, 149.1, 143.7, 136.3, 132.9, 130.5, 129.8, 129.1, 127.6, 126.0, 46.2, 41.5, 25.8, 24.9, 23.9, 21.2 ppm. The NMR data matched those reported in the literature.[S11] **ESI HRMS** *m/z* $C_{20}H_{23}N_3O_3S$ $[M+H]^+$: calcd 386.1533. Found: 386.1531. **IR (neat):** ν_{max} 3009, 2945, 2860, 2792, 1619 cm^{-1}. MP: 190.7-192.6 °C (literature:[S11] 191 °C).

2.3 Additional experimental data

2.3.1 Continuous-flow preparation of TsN_3 in a biphasic system

As an alternative to the conditions reported in the manuscript, the preparation of TsN_3 was implemented under biphasic continuous flow conditions (Figure S12) by mixing streams of aqueous sodium azide (1.5 M, 25 µL min^{-1}) and tosyl chloride in toluene (1.0 M, 25 µL min^{-1}). Process and reaction parameters such as temperature and residence time, as well as the presence of a phase transfer catalyst were optimized (Table S1, entries 1-8). Without phase transfer catalyst (entries 1-3), the conversion reached a mere 6% at 30 °C with a residence time of 10 min. Increasing the temperature to 90 °C led to 30% conversion in TsN_3. Mixing efficiency was assessed by using arrow-head micromixers rather than T-mixers and by increasing the flow rates, but it did not significantly impact on the conversion either. The

addition of a phase transfer catalyst (nBu$_4$NCl) significantly increased the reaction efficiency, with complete conversion at 90 °C in the presence of nBu$_4$NCl (10 mol%) with a residence time of 20 min (entry 8). A membrane separator was implemented downstream to remove the aqueous waste from the organic stream containing essentially pure TsN$_3$ (in-line control with IR; off-line control with ^{1}H NMR).

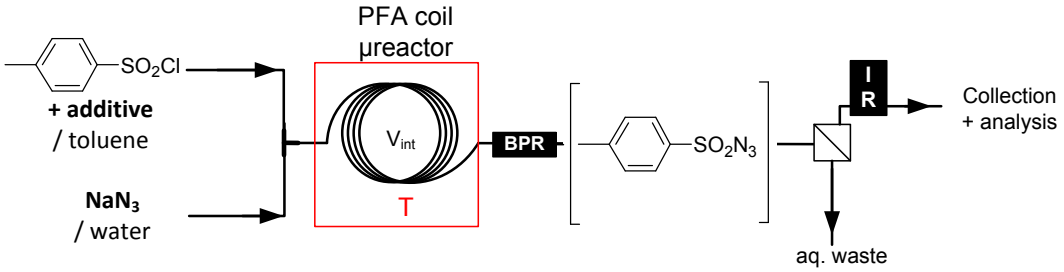

Figure S12. Preparation of TsN$_3$ under biphasic continuous-flow conditions

Table S1. Optimization of the preparation of TsN$_3$ under biphasic continuous-flow conditions

Entry	NaN$_3$ (M)	NaN$_3$/TsCl ratio	Additive (mol%)	T (°C)	Residence time (min)	Conv. (%)
1	NaN$_3$ (1.5)	1.5:1	-	30	10	6
2	NaN$_3$ (1.5)	1.5:1	-	60	10	11
3	NaN$_3$ (1.5)	1.5:1	-	90	10	30
4	NaN$_3$ (1.5)	1.5:1	nBu$_4$NCl (1)	30	10	13
5	NaN$_3$ (1.5)	1.5:1	nBu$_4$NCl (1)	60	10	29
6	NaN$_3$ (1.5)	1.5:1	nBu$_4$NCl (1)	90	10	72
7	NaN$_3$ (1.5)	1.5:1	nBu$_4$NCl (1)	90	20	87
8	NaN$_3$ (1.5)	1.5:1	nBu$_4$NCl (10)	90	20	quant.

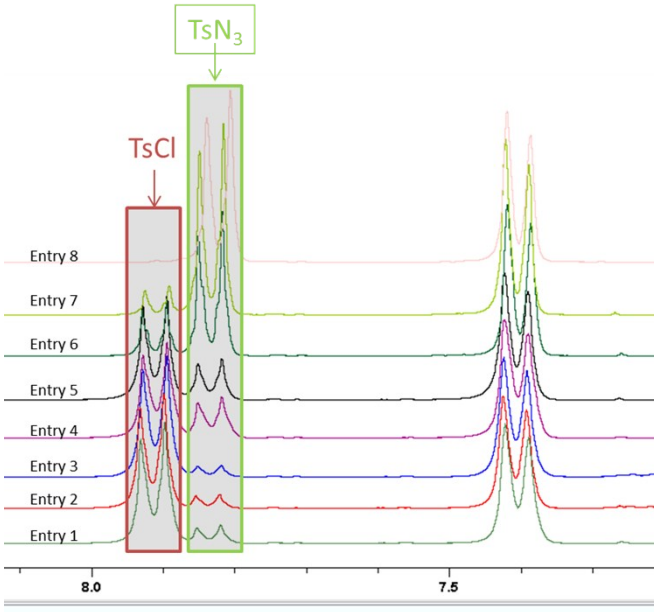

Figure S13. ^{1}H NMR reaction monitoring (off-line, 250 MHz): preparation of TsN_3 under biphasic continuous-flow conditions (see **Table S1**)

2.3.2 In-line reaction monitoring for the continuous-flow production of TsN_3

In-line reaction monitoring was carried out with a FlowIR™ (SN# 2964) from Mettler-Toledo with a DTGS detector using HappGenzel apodization, equipped with a SiComp (Silicon) probe connected via a FlowIR™ sensor. Sampling was performed from 4000 to 650 cm^{-1} at 8 wavenumber resolution with 208 scans. Figures S14 and S15 illustrate IR libraries for the biphasic (toluene/water) and for the homogeneous (NMP) continuous-flow preparation of tosyl azide, respectively.

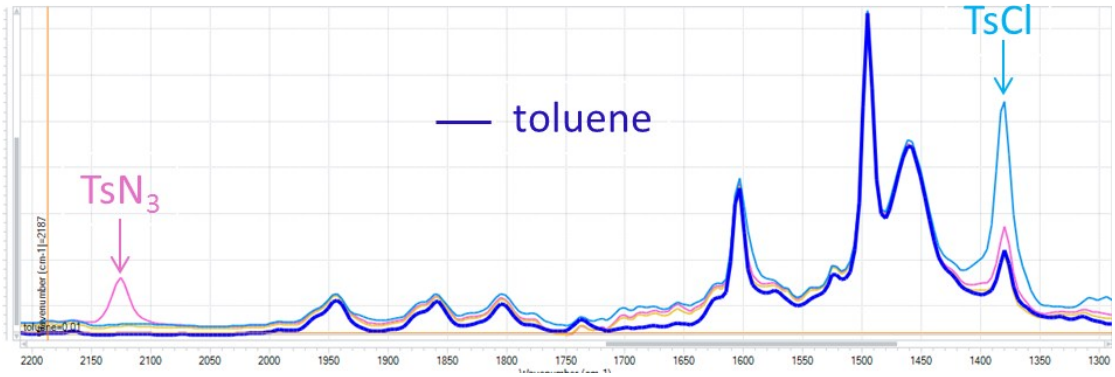

Figure S14. IR library utilized for the in-line qualitative reaction monitoring (toluene permeate)

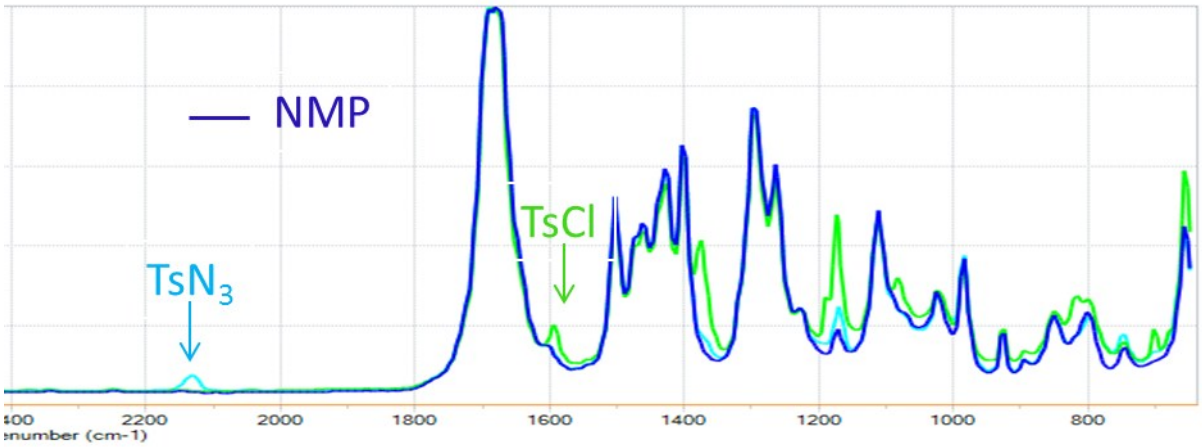

Figure S15. IR library utilized for the in-line qualitative reaction monitoring (in NMP)

2.3.3 Batch optimization of the diazo transfer reaction on methyl phenylacetate (**2a**)

General procedure: A solution of the selected base (1.5 eq) was added dropwise to a solution of methyl phenylacetate (1 mmol, 1 eq.) in the presence of the diazo transfer reagent (1.2 eq.) in the selected solvent (10 mL) at room temperature. The reaction mixture was reacted for 24 h. After extraction, removal of the water-soluble products and

concentration, the crude material was purified by chromatography on silica gel (petroleum spirit 40-60/diethyl ether 19:1).

Table S2. Optimization of the diazo transfer reaction on methyl phenylacetate (**2a**)

Entry	Azide	Solvent	Base	Conv.[a] (%)	Yield[b] (%)
1	tosyl azide	MeCN	DBU	75	66
2	*p*-acetamidobenzenesulfonyl azide	MeCN	DBU	65	53
3	diphenylphosphoryl azide	MeCN	DBU	0	0
4	benzotriazol-1-yl-sulfonyl azide	MeCN	DBU	22	16
5	tosyl azide	NMP	DBU	93	76
6	tosyl azide	NMP/H_2O 2:1	DBU	> 99	74
7	tosyl azide	propylene carbonate	DBU	82	56
8	tosyl azide	DMSO	DBU	> 99	69
9	tosyl azide	DMSO/H_2O 2:1	DBU	> 99	61
10	tosyl azide	THF	DBU	10	8
11	tosyl azide	toluene	DBU	6	3
12	tosyl azide	toluene	*n*-BuLi	17	14
13	tosyl azide	NMP	$CaCO_3$	0	0
14	tosyl azide	NMP	Cs_2CO_3	18	15
15	tosyl azide	NMP	K_2CO_3	64	43
16	tosyl azide	NMP	pyridine	0	0
17	tosyl azide	NMP	DABCO	0	0
18	tosyl azide	NMP	NEt_3	0	0
19	tosyl azide	NMP	TMG	87	66
20	tosyl azide	NMP	Amber.® A26	35	18
21	tosyl azide	NMP	Amber.® A21	25	21
22	tosyl azide	NMP	P_2-Et	> 99	71
23	tosyl azide (1.5 eq.)	NMP	DBU	> 99	84

[a] Determined by ^{1}H NMR. [b] Isolated yield after purification by column chromatography.

2.3.4 Batch optimization of catalyzed C-H carbene insertion of methyl phenyldiazoacetate (**4a**) and *N*-Boc piperidine (**3a**)

General procedure: the catalyst (5 mol% or 1 mol%), *N*-Boc piperidine (4 eq.) and dry hexane were successively added to a flame-dried two-neck round-bottom flask under an argon atmosphere. The mixture was degassed under an argon flow for 10 min. A solution of methyl phenyldiazoacetate (1.70 mmol, 1 eq.) in dry and degassed hexane (5 mL) was next added dropwise over a 3 h period at room temperature under argon. After complete addition, the mixture was stirred for an additional 12 h. The crude mixture was analyzed by HPLC. The reaction mixture was filtered over celite, the solvent was removed under reduced pressure and the resulting crude material was purified by column chromatography on neutralized silica gel (petroleum spirit 40-60/diethyl ether 9:1) to give *N*-Boc methylphenidate (**5a**) as an oil. The *threo*/*erythro* ratio was calculated by ^{1}H NMR in $CDCl_3$ (using the two singlets at 3.63 and 3.68 ppm, and the two multiplets at 2.92-3.15 and 2.64-2.78 ppm, see Figure S16).

Table S3. Optimization of catalyzed C-H carbene insertion of methyl phenyldiazoacetate (**4a**) and *N*-Boc piperidine (**3a**)

Entry	**Catalyst**	**Yield**[a] (%)	***Threo/Erythro***[b]
1	$Rh_2(OAc)_4$	37	3.5:1
2	$Rh_2(CF_3COO)_4$	46	1.2:1
3	Rh_2(heptafluorobutyrate)$_4$	30	2.4:1
4	$Rh_2(oct)_4$	60	3:1
5[c]	$Rh_2(oct)_4$	45	2.8:1
6[d]	$Rh_2(oct)_4$	35	2:1
7	$Rh_2(esp)_2$	54	1.9:1
8	Cu(8-hydroxyquinolate)$_2$	0	-
9	$Cu(OTf)_2$	0	-
10	$Cu(acac)_2$	0	-
11[e]	-	0	-

[a] Isolated yield after purification by column chromatography. [b] Determined by ^{1}H NMR. [c] 1 mol% of catalyst was used. [d] The reaction was performed in DCM. [e] Irradiation @ 395 nm for 4 h, 1 equivalent of *N*-Boc piperidine (**3a**) was employed.

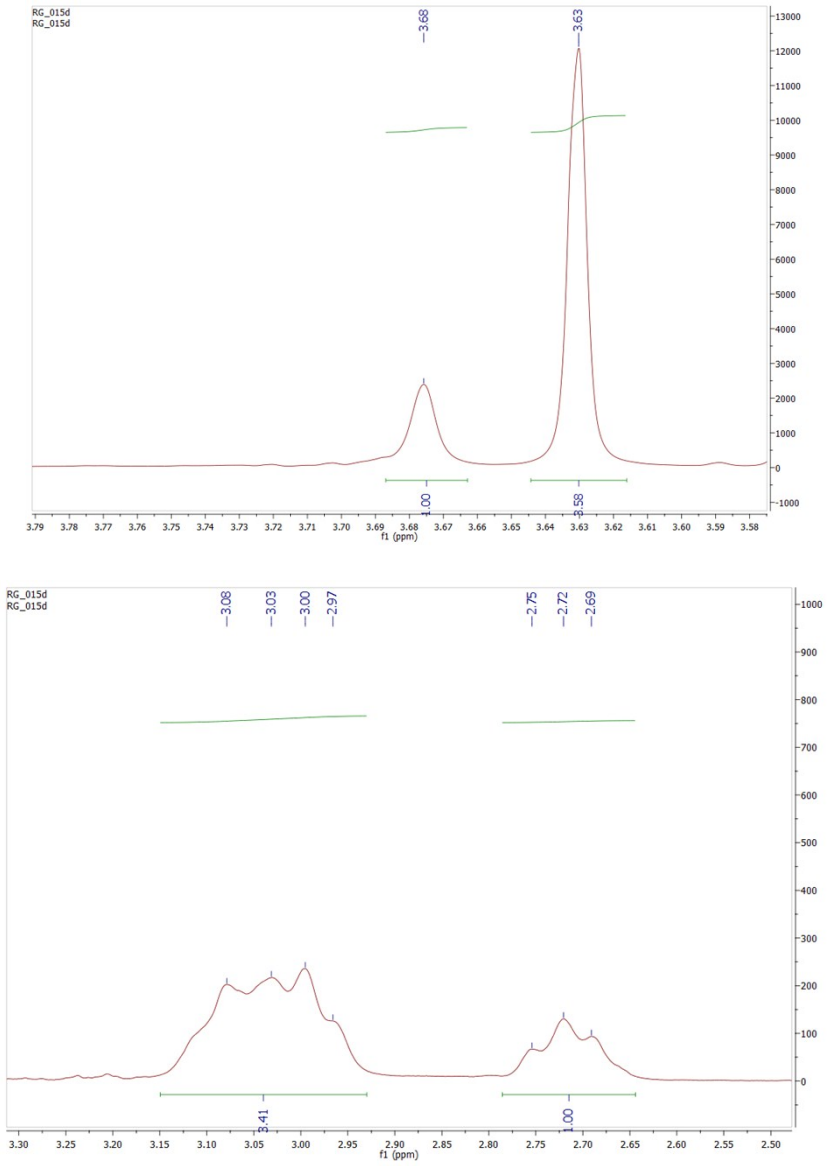

Figure S16. ^{1}H NMR peaks used to calculate the *threo/erythro* ratio of compound **5a**

2.3.5 Off-line deprotection of *N*-Boc-methylphenidate (**5a**)

5a (0.24 mmol, 1 eq.) was dissolved in dichloromethane, and TFA (10 eq.) was added dropwise under stirring at room temperature. The resulting mixture was stirred for 3 additional hours. The solvent was removed under reduced pressure, and the crude was dissolved in 25 mL of water (acidified with 1 drop of aqueous HCl 37%). The pH of the aqueous phase was adjusted to 10-11 with Na_2CO_3, and the aqueous phase was extracted with 3 x 25 mL of CH_2Cl_2. The organic layers were dried over sodium sulfate, filtered, and 4 mL of HCl 1 M in Et_2O were added. The resulting mixture was stirred for 5 min at room temperature, and the solvent was removed under reduced pressure to give methylphenidate hydrochloride (**1**·HCl) as a white solid in quantitative yield and with retention of stereochemistry.

2.3.6 Preliminary screening of the thermolysis and photolysis of hydrazone **3b** towards β-lactam **5b**

General procedure: A solution of tosylhydrazone (0.78 mmol, 1 eq.) in the appropriate solvent or solvent mixture was treated with the selected base (1.1 eq.). The resulting reaction mixture was next irradiated at 395 nm for 18 h or thermolyzed towards the formation of β-lactam **5b.** After extraction of water-soluble impurities and solvent evaporation, the conversion and *threo/erythro* ratio were determined by ^{1}H NMR (using the doublet at 4.61 ppm and the peaks at 3.37 and 2.18 ppm, see Figure S17).

Table S4. Batch screening of the thermolysis and photolysis of hydrazone **3b** towards β-lactam **5b**

Entry	Base	Solvent	T/Irradiation/Catalyst	Conv.[a] (%)	*Threo/Erythro*[a]
1	*t*BuOK	toluene	395 nm	> 99	4.6:1
2	*t*BuOK	toluene/propylene carbonate 3:1	395 nm	> 99	4.4:1
3	*t*BuOK	propylene carbonate	395 nm	> 99[b]	-[c]
4	*t*BuOK	MeCN	395 nm	> 99	3.1:1
5	*t*BuOK	THF	395 nm	> 99	4.1:1
6	NEt_3	toluene	395 nm	65	4.4:1
7	DBU	toluene	395 nm	> 99	4.8:1
8	DBU	DCM/MeCN 9:1	395 nm	93	5.9:1
9	DBU	NMP	395 nm	> 99	2.7:1
10	DBU	MeOH	395 nm	0	-
11	-	toluene	395 nm	0	-
12	DBU	toluene	120 °C[d]	> 99	3.9:1
13	KOH	toluene/H_2O 2:1	90 °C[d]	> 99	4:1
14	KOH[e]	toluene/H_2O 2:1	90 °C[d]	> 99	4.3:1
15	*t*BuOK	EtOH	90 °C[d]	0	-
16[f]	*t*BuOK	toluene	$Rh_2(OAc)_4$ + 90 °C	0	-

[a] Determined by ^{1}H NMR. [b] Determined by HPLC. [c] Not calculated. [d] Heating for 4 h. [e] Reaction conducted in the presence of 10 mol% of Aliquat® 336. [f] Heating for 3 h, 3 equivalents of base were used.

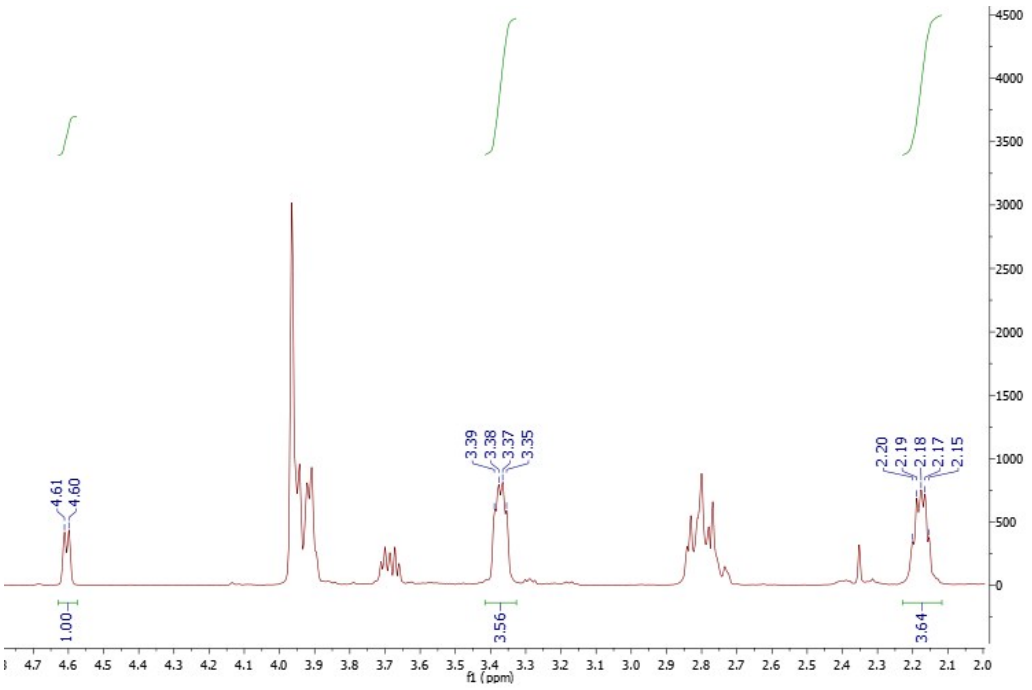

Figure S17. ^{1}H NMR peaks used to calculate the *threo/erythro* ratio of compound **5b**

2.3.7 Thermolysis *vs* photolysis of hydrazone **3b** towards β-lactam **5b** in a batch setup

General procedure (batch): 100 mL of a 0.75 M solution of tosylhydrazone **3b** in the presence of Aliquat® 336 (10 mol%) and DBU (1.1 eq.) in toluene was thermolyzed at 120 °C or irradiated at 395 nm at 35 °C. Samples were analyzed by ^{1}H NMR.

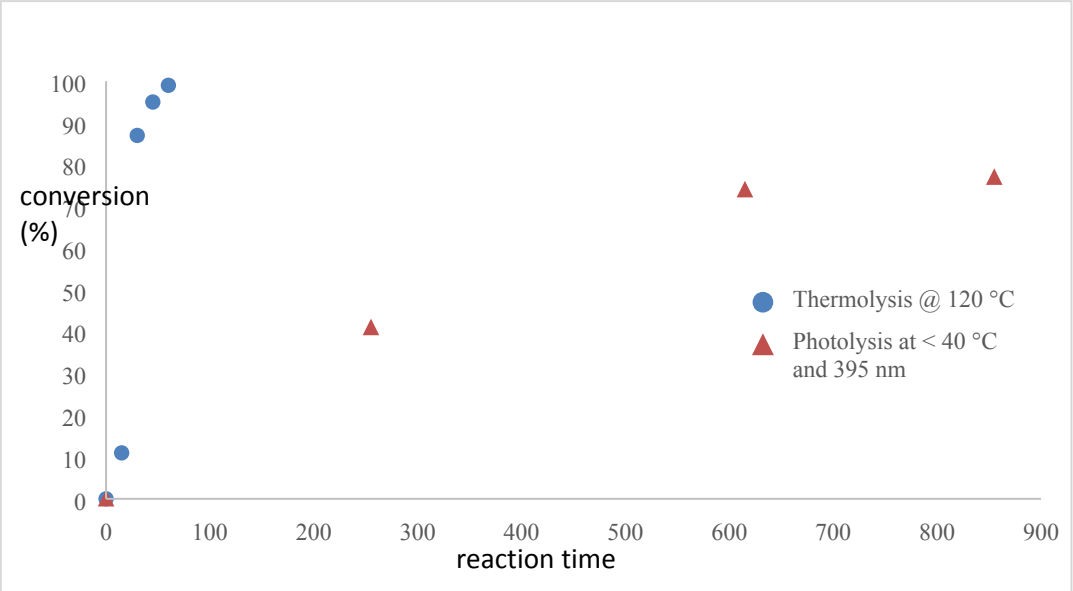

Figure S18. Conversion *vs* reaction time for the thermolysis and photolysis of hydrazone **3b** (in batch)

Table 5 illustrates the evolution of the *threo*/*erythro* ratio as a function of time (batch mode, see details above). A higher *threo*/*erythro* ratio was observed at the beginning of the reaction (low conversion), and the *threo*/*erythro* ratio plateaued at 3.7:1 after 45 min of thermolysis (up to complete conversion).

Table S5. Conversion and stereoselectivity as a function of the reaction time for the thermolysis of hydrazone **3b** (batch mode)

Entry	Reaction time (min)	Conversion (%) [a]	*Threo*/*Erythro* [a]
1	0	0	-
2	15	11	5.8:1
3	30	87	3.8:1
4	45	95	3.7:1
5	60	>99	3.7:1

[a] Determined by ^{1}H NMR

2.3.8 Off-line purification of methylphenidate hydrochloride (**1**·HCl)

2.3.8.1 Liquid-liquid extraction

The effluent of the reactor was collected for 67 min, and the solvent was removed under reduced pressure. Aqueous HCl (150 mL, 0.04 M) was added and, the resulting mixture was stirred for 10 min at room temperature and filtered. The pH of the filtrate was adjusted to 10-11 with sodium carbonate, and the solution washed with CH_2Cl_2 (3 x 50 mL). The combined organic layers were dried over Na_2SO_4 and filtered. Finally, 10 mL of a 1 M solution of HCl in diethyl ether were added, the mixture was stirred for 5 min at room temperature and then evaporated under reduced pressure. This gave methylphenidate hydrochloride (**1**·HCl) as a white solid (944 mg, 70%), in a 2.2:1 *threo/erythro* ratio (^{1}H NMR ratio in D_2O).

2.3.8.2 Recrystallization

An analytical sample of the racemate *threo*-methylphenidate hydrochloride (**1a,b**·HCl) could be obtained by recrystallization from *sec*-butanol/diethyl ether (2:1). The racemate **1a,b**·HCl was characterized by NMR (section 2.5) and chiral HPLC (section 2.6).

2.3.9 Cost estimate for the inter- and intramolecular strategies

The costs associated with the reactants and reagents for the inter- and intramolecular processes were assessed, including the preparation of all chemical intermediates (Tables S6-S7). Reactant and reagent sale prices were gathered from chemical suppliers (kilogram scale, reagent grades). Solvents were excluded (reaction and purification solvents), as well as the costs related to electric energy consumption. The costs associated with the additional purification strategies necessary to reach pharmaceutical quality in the final product, and to separate the *threo* and *erythro* forms were not taken into account.

Table S6. Cost estimate for the intermolecular strategy

Reactant	Catalog Price	Quantity/g[a]	Cost/g[a] (€)	Cost percentage
TsCl	202.5 € (3 kg)	2.91 g	0.20	0.5
NaN_3	457.5 € (2 kg)	2.95 g	0.68	1.7
NBu_4OH 40% in H_2O	818 € (2.5 kg)	14.8 g	4.85	11.9
Phenylacetic acid	50.7 € (500 g)	1.74 g	0.17	0.4
DBU	337 € (500 g)	2.14 g	1.45	3.5
Boc_2O	377 € (500 g)	10.27 g	7.75	19
Piperidine	235.5 € (1 L)	5.15 mL	0.80	2
$Rh_2(oct)_4$	157 € (500 mg)	77 mg	24.09	58.9
TFA	614 € (2 L)	2.84 mL	0.87	2.1
Total			40.86 € (**59.43 €**)[b]	

[a] Quantity and cost necessary to produce 1 g of **1**·HCl (sequential flow process). [b] The cost in parentheses is the cost necessary to produce 1 g of *threo*-**1**·HCl, which was obtained by dividing the total reactants cost by the percentage of *threo*-compound recovered within the final product.

Table S7. Cost estimate for the intramolecular strategy

Reactant	Catalog Price	Quantity/g[a]	Cost/g[a] (€)	Cost percentage
methyl benzoylformate	327 € (500 g)	1.21 g	0.79	27.8
piperidine	235.5 € (1 L)	0.73 mL	0.17	6
$TsNHNH_2$	173.5 € (500 g)	1.26 g	0.44	15.5
$TsOH.H_2O$	89.3 € (3 kg)	76 mg	< 0.01	< 0.1
Aliquat® 336	76.7 € (1 L)	0.27 mL	0.02	0.7
DBU	337 € (500 g)	0.89 g	0.6	21.1
HCl 4 M in dioxane	115 € (500 mL)	3.55 mL	0.82	28.9
Total			2.84 € (**4.13 €**)[b]	

[a] Quantity and cost necessary to produce 1 g of **1**·HCl. [b] The cost in parentheses is the cost necessary to produce 1 g of *threo*-**1**·HCl, which was obtained by dividing the total reactants cost by the percentage of *threo*-compound recovered within the final product.

2.4 NMR data and characterization of representative compounds prepared by continuous-flow strategies

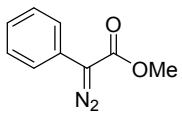

$C_9H_8N_2O_2$
Mol. Wt.: 176.17

Methyl phenyldiazoacetate (4a). **^{1}H NMR ($CDCl_3$, 400 MHz):** δ = 7.48 (d, J = 7.5 Hz, 2H), 7.38 (t, J = 7.9 Hz, 2H), 7.18 (t, J = 7.4 Hz, 1H), 3.86 (s, 3H) ppm. **^{13}C NMR ($CDCl_3$, 100.6 MHz):** δ = 165.6, 128.9, 125.8, 125.5, 124.0, 52.0 ppm. The NMR data matched those reported in the literature.[S13] **ESI HRMS** *m/z* $C_9H_8N_2NaO_2^+$ $[M+Na]^+$: calcd 199.0478. Found: 199.0477. **IR (neat):** ν_{max} 2953, 2081, 1698 cm^{-1}.

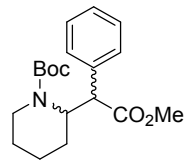

$C_{19}H_{27}NO_4$
Mol. Wt.: 333,43

***N*-Boc methylphenidate (5a).** 3:1 mixture of *threo* and *erythro* isomers. **^{1}H NMR ($CDCl_3$, 400 MHz):** δ = 7.20-7.52 (m, 5H), 4.79-5.20 (brm, 1H), 4.10-4.24 (m, 1.25H), 3.95-4.10 (m, 0.75H), 3.68 (s, 0.75H), 3.63 (s, 2.25H), 2.92-3.15 (brm, 0.75H), 2.64-2.78 (brm, 0.25H), 1.32-1.80 (m, 13H), 1.24 (brs, 2H) ppm. **^{13}C NMR ($CDCl_3$, 100.6 MHz):** δ = 172.3, 154.5, 154.2, 136.3, 136.2, 129.0, 128.6, 128.3, 127.9, 127.6, 127.1, 79.6, 79.5, 54.3, 52.8, 52.0, 51.9, 51.5, 50.9, 39.8, 38.4, 29.0, 28.3, 28.0, 27.8, 27.6, 25.4, 25.3, 25.1, 19.2, 18.8 ppm. The NMR data matched those reported in the literature.[S14] **ESI HRMS** *m/z* $C_{19}H_{28}NO_4^+$ $[M+H]^+$: calcd 334.2013. Found: 334.2011. **IR (neat):** ν_{max} 2933, 2864, 1735, 1685 cm^{-1}.

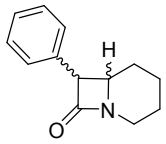

$C_{13}H_{15}NO$
Mol. Wt.: 201,27

7-Phenyl-1-aza-bicyclo[4.2.0]octan-8-one (5b). 3:1 mixture of *threo* and *erythro* isomers. **^{1}H NMR ($CDCl_3$, 400 MHz):** δ = 7.21-7.38 (m, 5H), 4.61 (d, *J* = 4.6 Hz, 0.25H), 3.87- 3.99 (m, 1.75H), 3.68 (m, 0.25H), 3.37 (dd, *J* = 9.1, 4.8 Hz, 0.75H), 2.70-2.86 (m, 1H), 2.18 (dt, *J* = 9.1, 4.7 Hz, 0.75H), 1.92 (brs, 0.75H), 1.80 (d, *J* = 11.5 Hz, 0.25H), 1.60-1.75 (m, 1H), 1.30-1.53 (m, 3H), 0.81-0.95 (m, 0.25H) ppm. **^{13}C NMR ($CDCl_3$, 100.6 MHz):** δ = 166.6, 166.2, 135.6, 133.5, 128.6, 128.4, 128.3, 127.2, 127.0, 63.4, 58.2, 56.7, 52.6, 38.9, 38.6, 30.4, 26.7, 24.8, 24.4, 22.1, 21.7 ppm. The NMR data matched those reported in the literature.[S11, S15] **ESI HRMS** *m/z* $C_{13}H_{16}NO^+$ $[M+H]^+$: calcd 202.1226. Found: 202.1227. **IR (neat):** ν_{max} 2943, 2896, 2858, 1728 cm^{-1}. **MP**: 65.4-68.8 °C (literature,[S11] *threo*-**5b**: 87 °C).

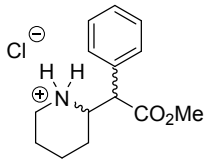

$C_{14}H_{20}ClNO_2$
Mol. Wt.: 269,77

***threo*-Methylphenidate hydrochloride (1a,b·HCl). ^{1}H NMR (D_2O, 400 MHz):** δ = 7.30 (d, *J* = 6.6 Hz, 3H), 7.17 (d, *J* = 6.3 Hz, 2H), 3.86 (d, *J* = 9.2 Hz, 1H), 3.68 (t, *J* = 10.1 Hz, 1H), 3.57 (s, 3H), 3.32 (d, *J* = 12.7 Hz, 1H), 2.94 (t, J = 12.8 Hz, 1H), 1.72 (d, *J* = 14.3 Hz, 1H), 1.63 (d, *J* = 11.4 Hz, 1H), 1.39-1.54 (m, 2H), 1.16–1.35 (m, 2H) ppm. **^{13}C NMR (D_2O, 100.6 MHz):** δ = 173.2, 133.3, 129.5, 128.9, 128.6, 57.8, 53.7, 53.2, 45.6, 26.2, 21.8, 21.3 ppm. The NMR data matched those reported in the literature.[S16] **ESI HRMS** *m/z* $C_{14}H_{20}NO_2^+$ $[M+H]^+$: calcd 234.1489. Found: 234.1488. **IR (neat):** ν_{max} 2934, 2804, 2703, 2512, 2413, 1738 cm^{-1}. **MP:** 218.4-219.8°C (literature:[S17] 221-223 °C for **1a**·HCl and 219-221 °C for **1b**·HCl).

2.5 Copies of ^{1}H and ^{13}C NMR spectra

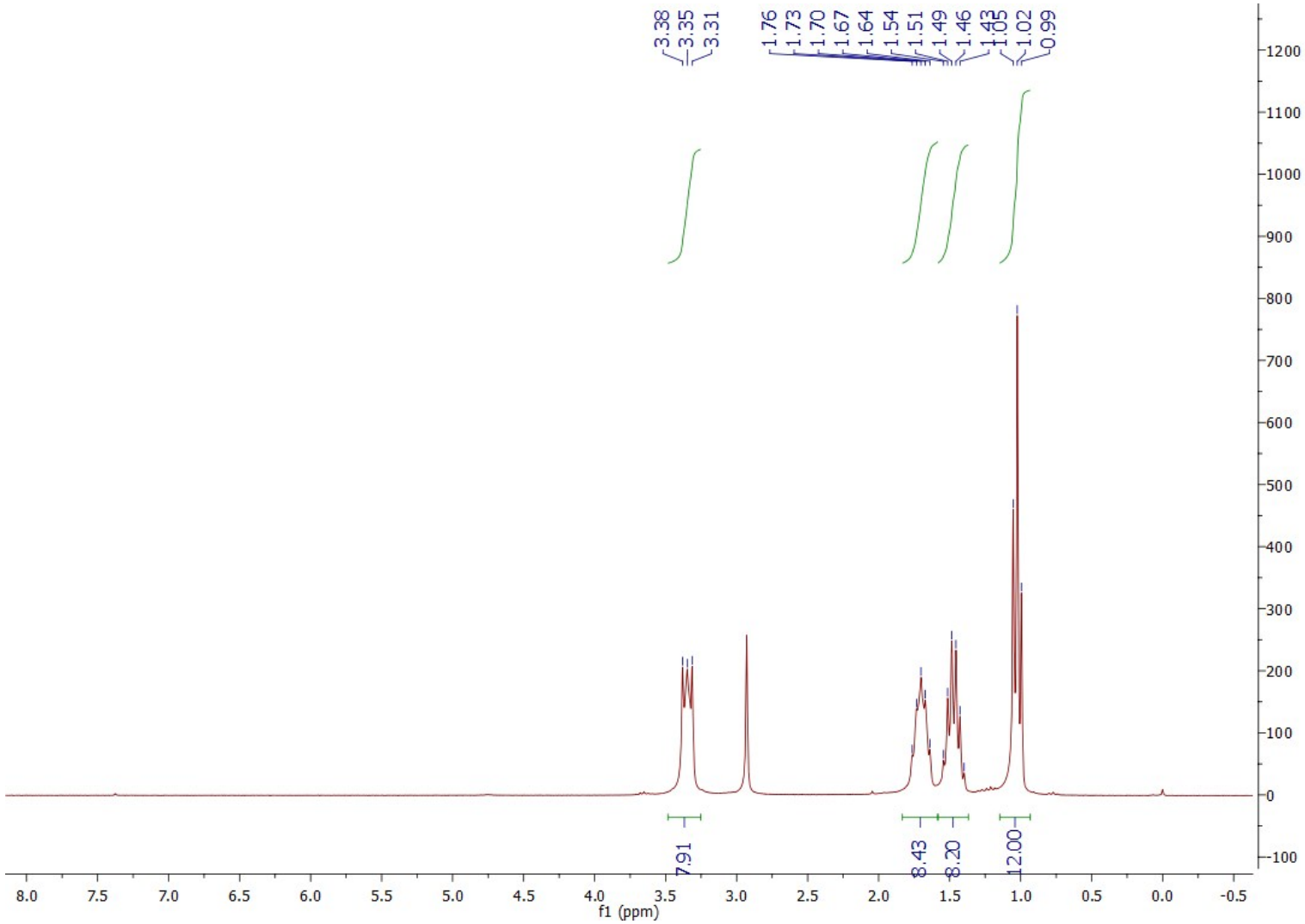

Figure S19. ^{1}H NMR spectrum (250 MHz) of tetrabutylammonium azide in $CDCl_3$

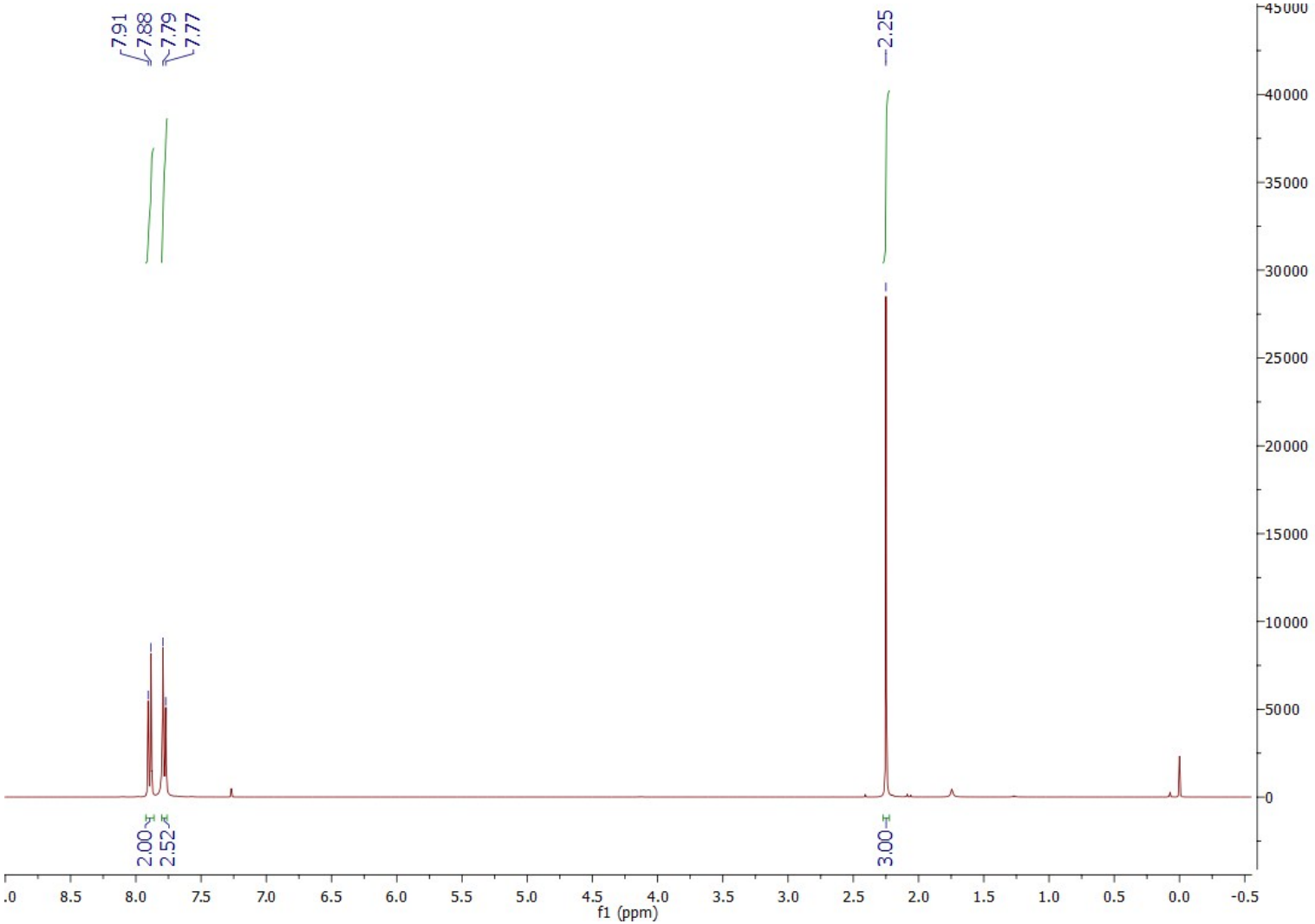

Figure S20. ^{1}H NMR spectrum (400 MHz) of *p*-acetamidobenzenesulfonyl azide in $CDCl_3$

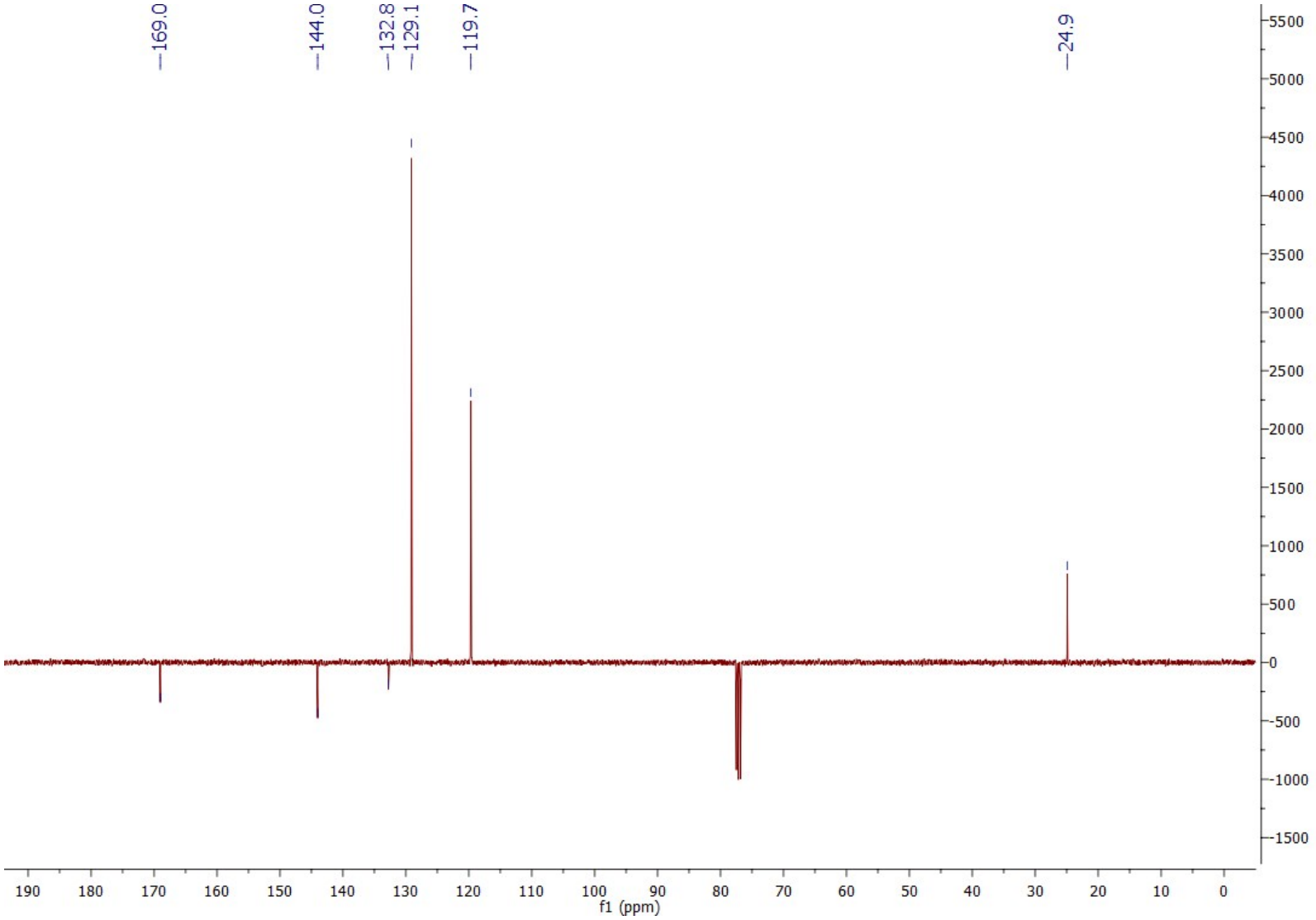

Figure S21. ^{13}C APT NMR spectrum (100.6 MHz) of *p*-acetamidobenzenesulfonyl azide in $CDCl_3$

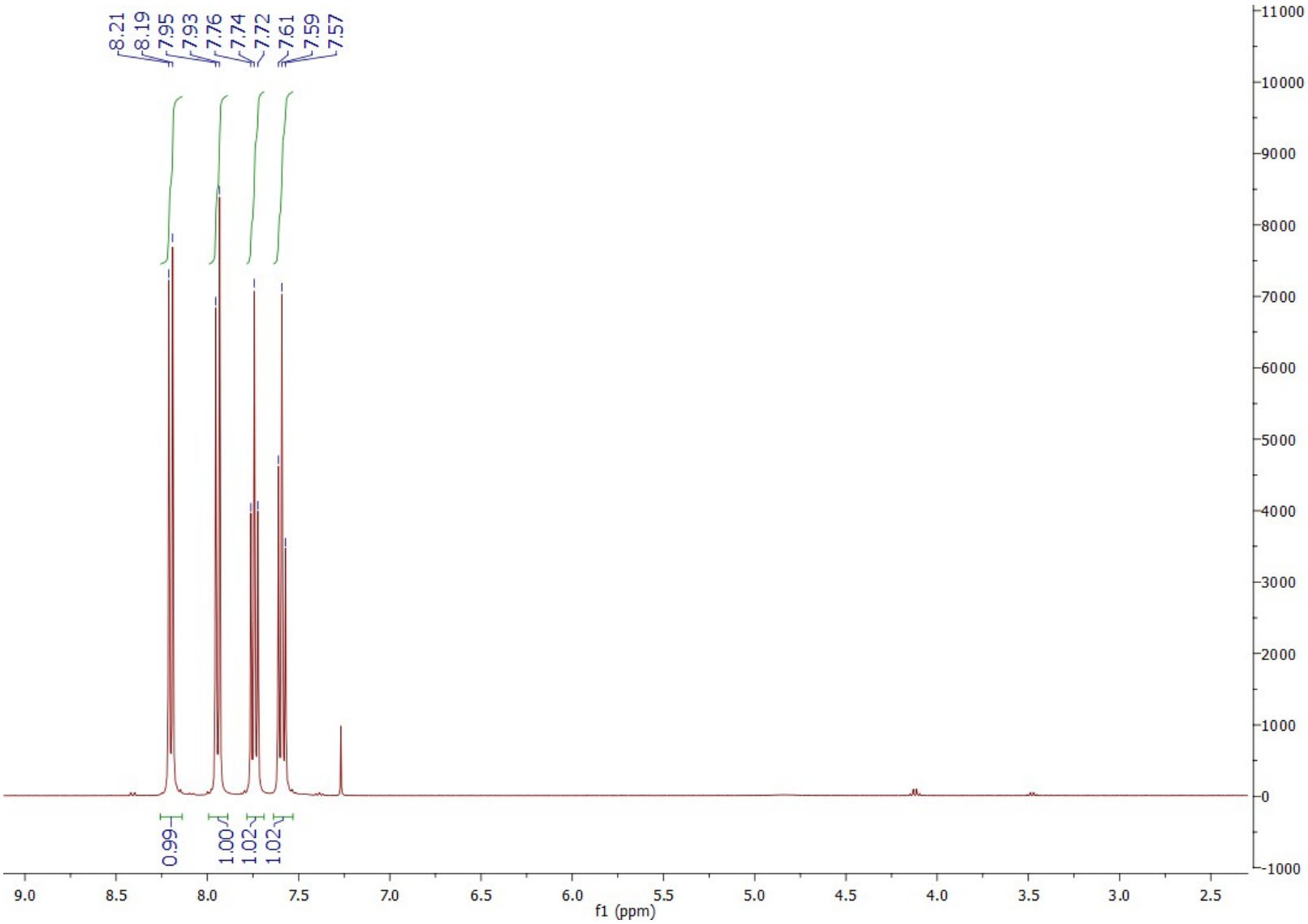

Figure S22. ^{1}H NMR spectrum (400 MHz) of benzotriazol-1-yl-sulfonyl azide in $CDCl_3$

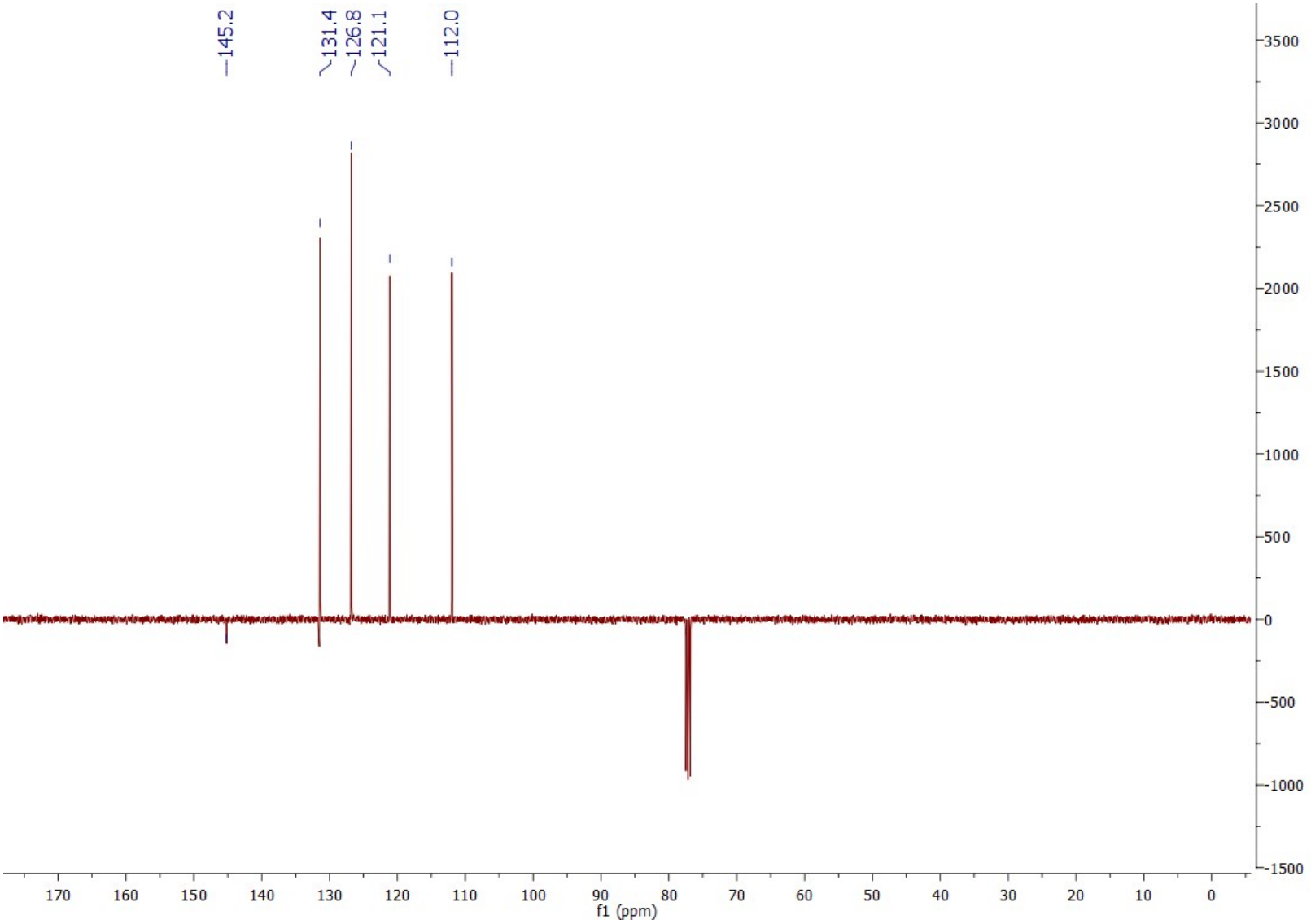

Figure S23. ^{13}C NMR APT spectrum (100.6 MHz) of benzotriazol-1-yl-sulfonyl azide in $CDCl_3$

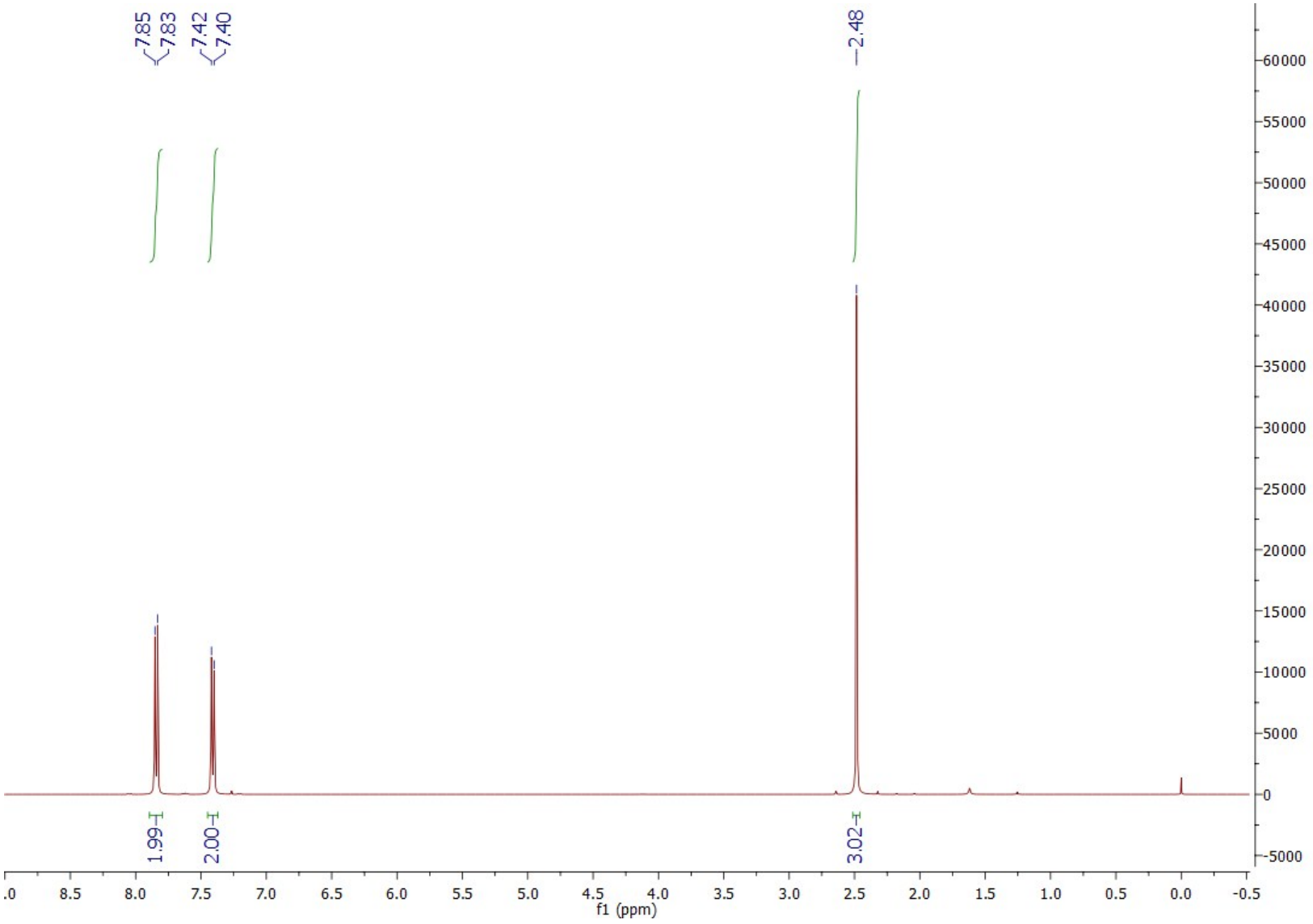

Figure S24. ^{1}H NMR spectrum (400 MHz) of *p*-toluenesulfonyl azide in $CDCl_3$

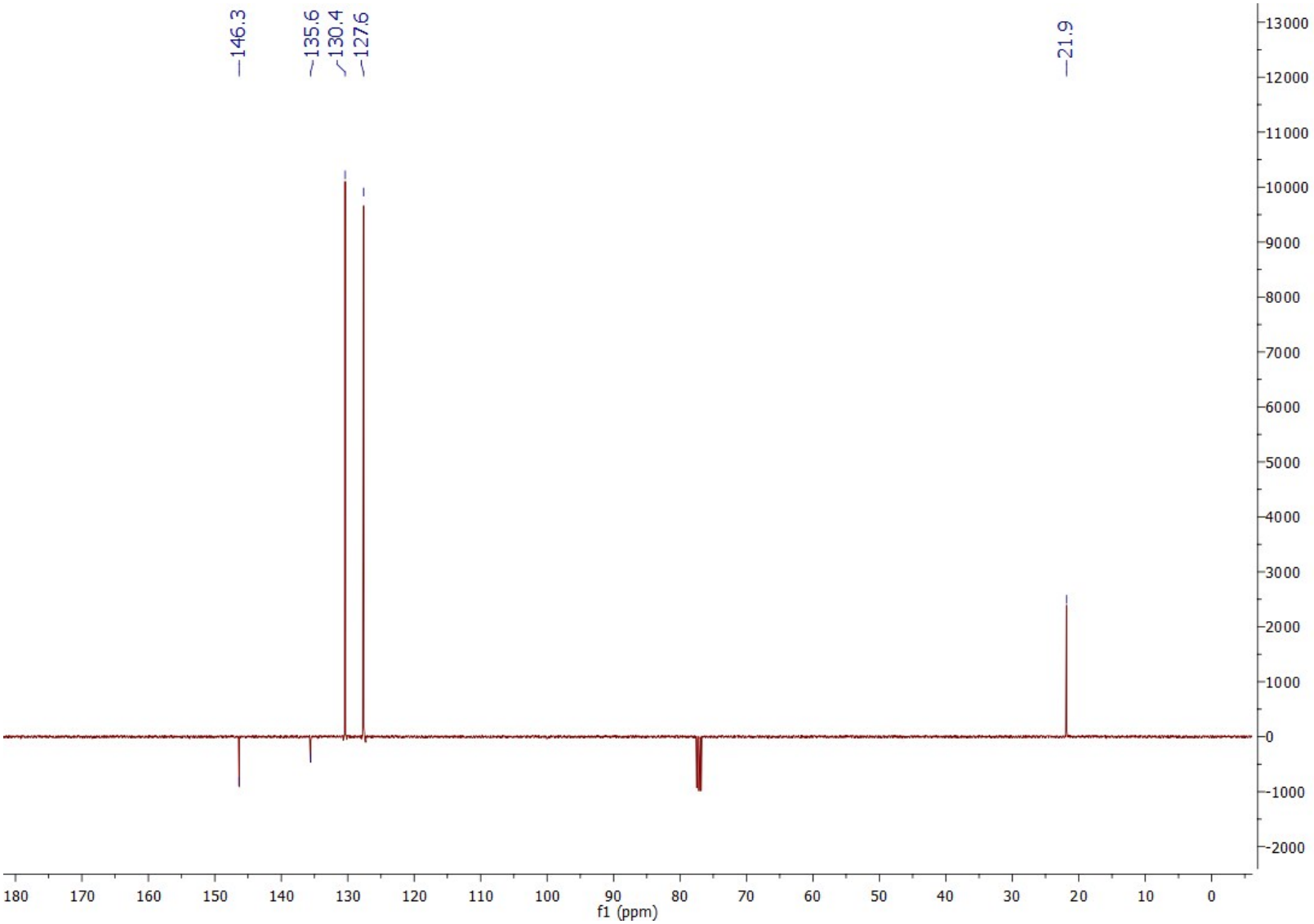

Figure S25. ^{13}C APT NMR spectrum (100.6 MHz) of *p*-toluenesulfonyl azide in $CDCl_3$

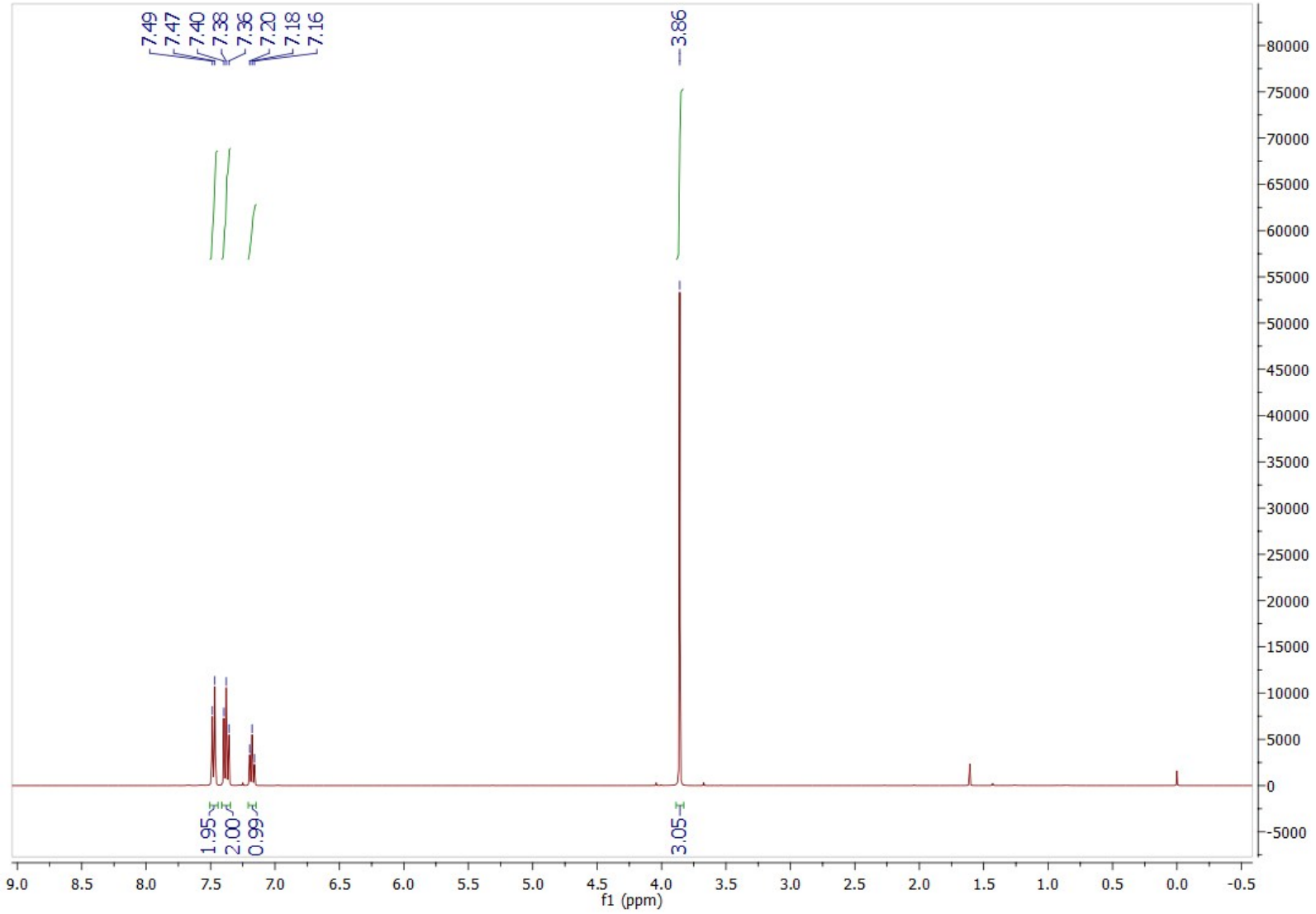

Figure S26. ^{1}H NMR spectrum (400 MHz) of methyl phenyldiazoacetate (**4a**) in $CDCl_3$

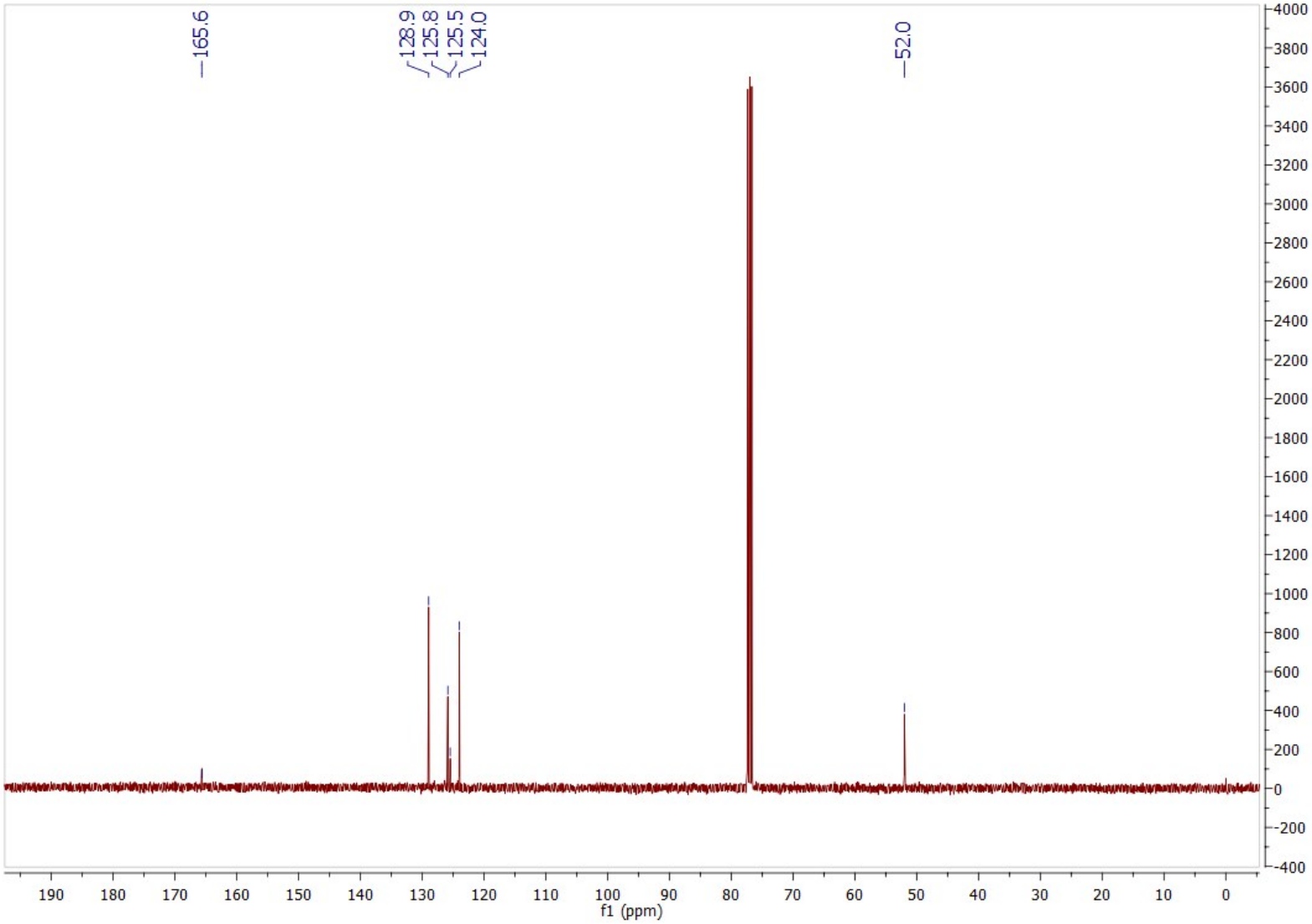

Figure S27. ^{13}C NMR spectrum (100.6 MHz) of methyl phenyldiazoacetate (**4a**) in $CDCl_3$

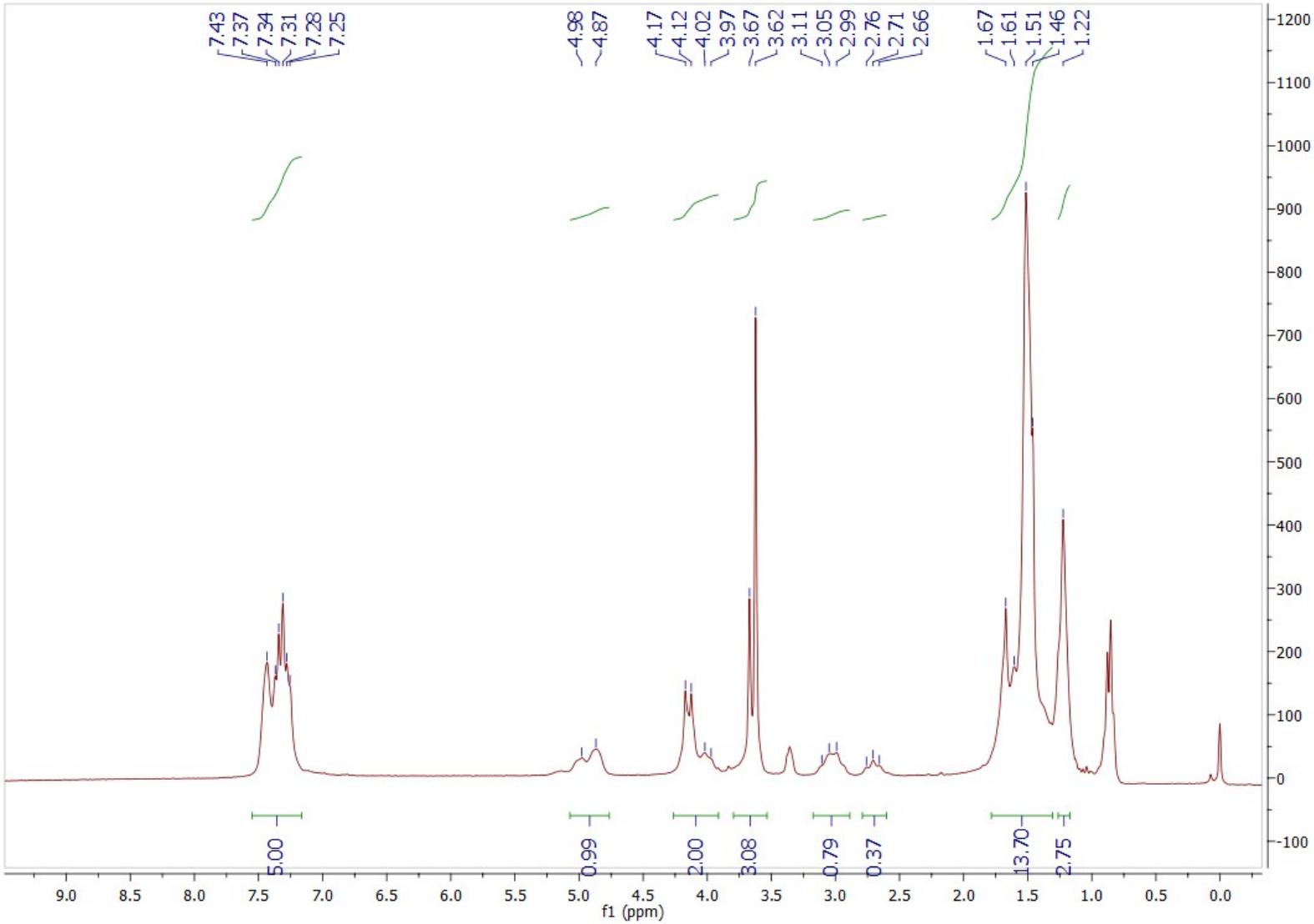

Figure S28. ^{1}H NMR spectrum (250 MHz) of *N*-Boc-methylphenidate (**5a**, mixture of 3:1 *threo* and *erythro* isomers) in $CDCl_3$

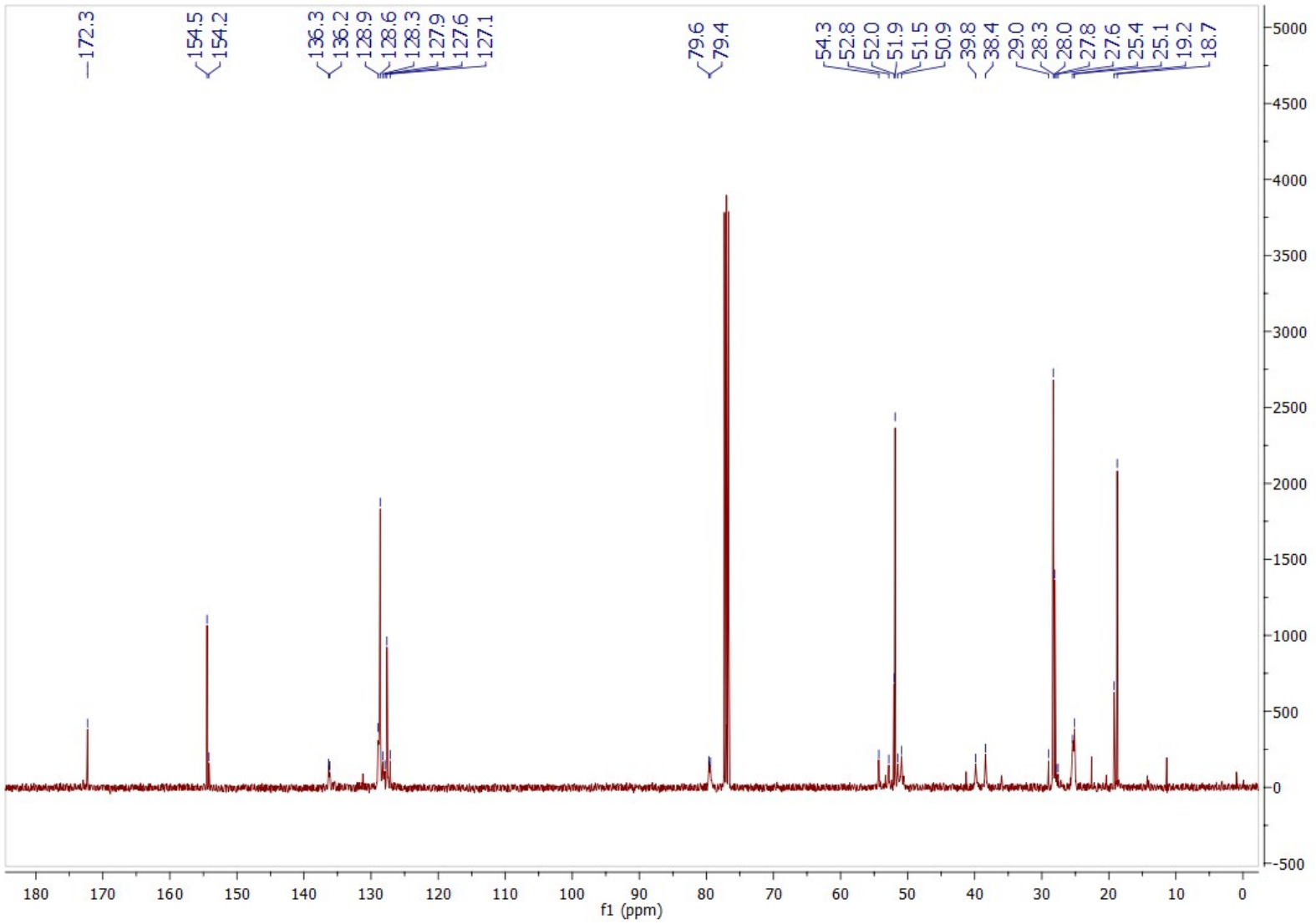

Figure S29. ^{13}C NMR spectrum (100.6 MHz) of *N*-Boc-methylphenidate (**5a**, mixture of 3:1 *threo* and *erythro* isomers) in $CDCl_3$

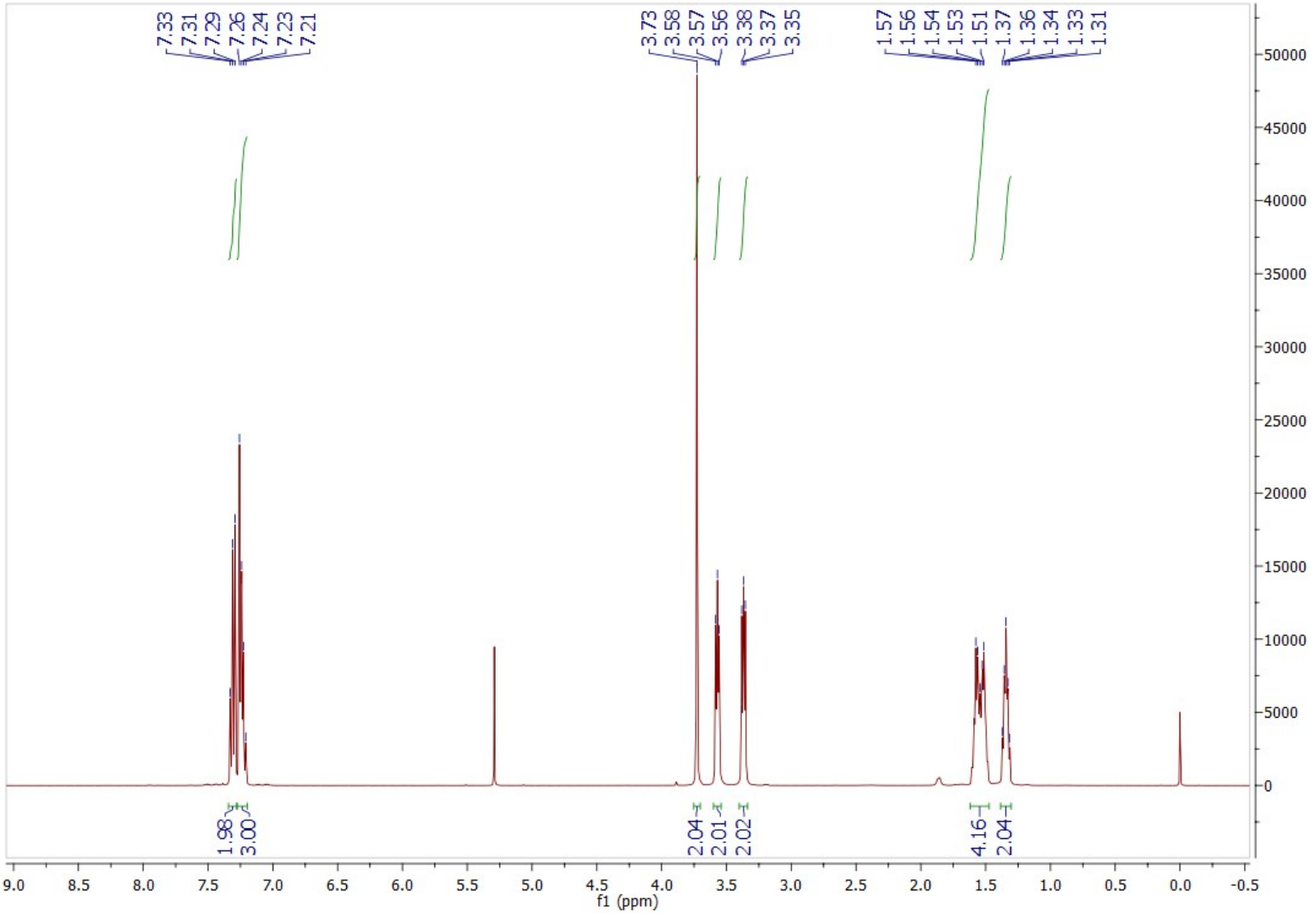

Figure S30. ^{1}H NMR spectrum (400 MHz) of 2-phenyl-1-(piperidin-1-yl)ethanone in $CDCl_3$

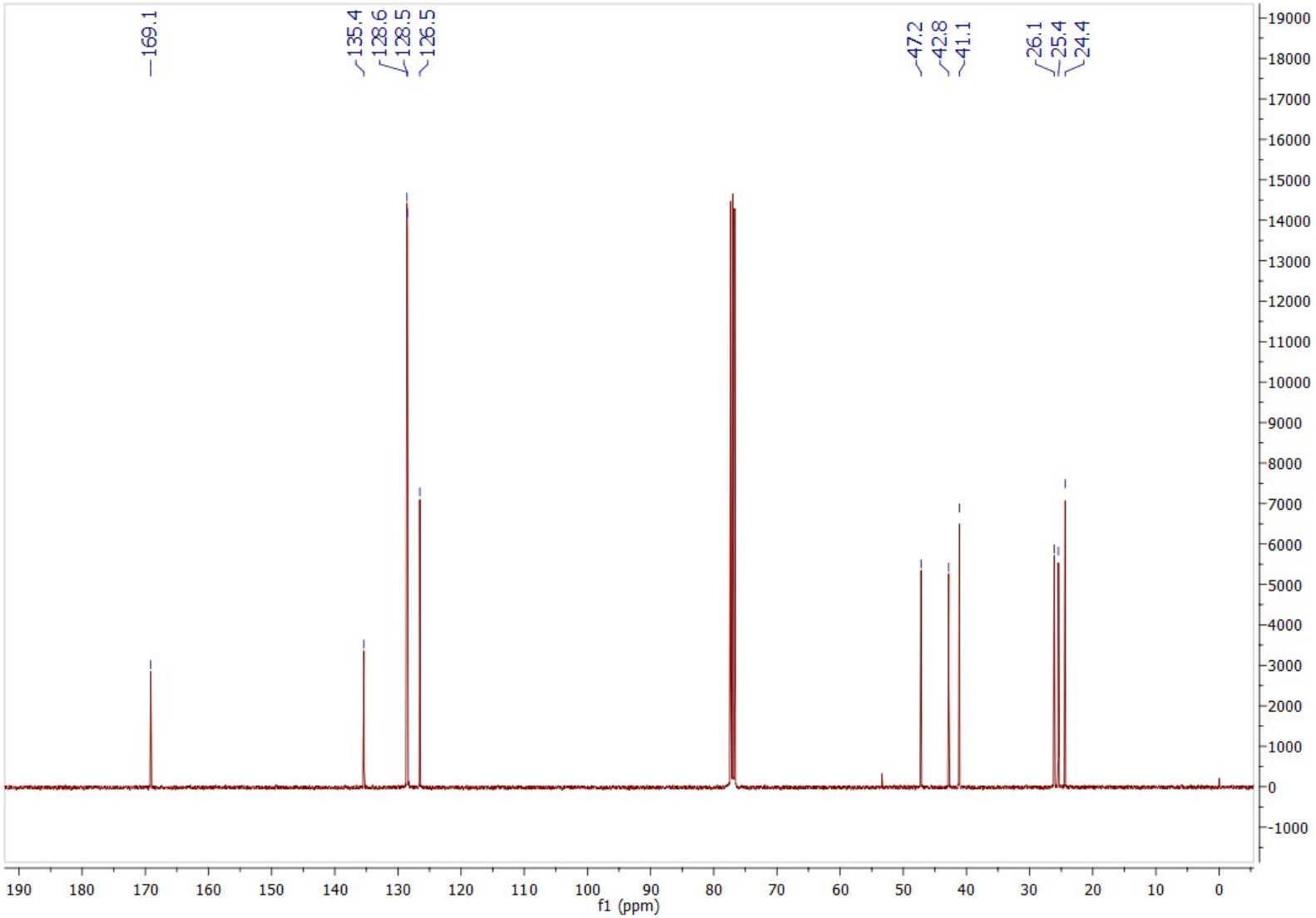

Figure S31. ^{13}C NMR spectrum (100.6 MHz) of 2-phenyl-1-(piperidin-1-yl)ethanone in $CDCl_3$

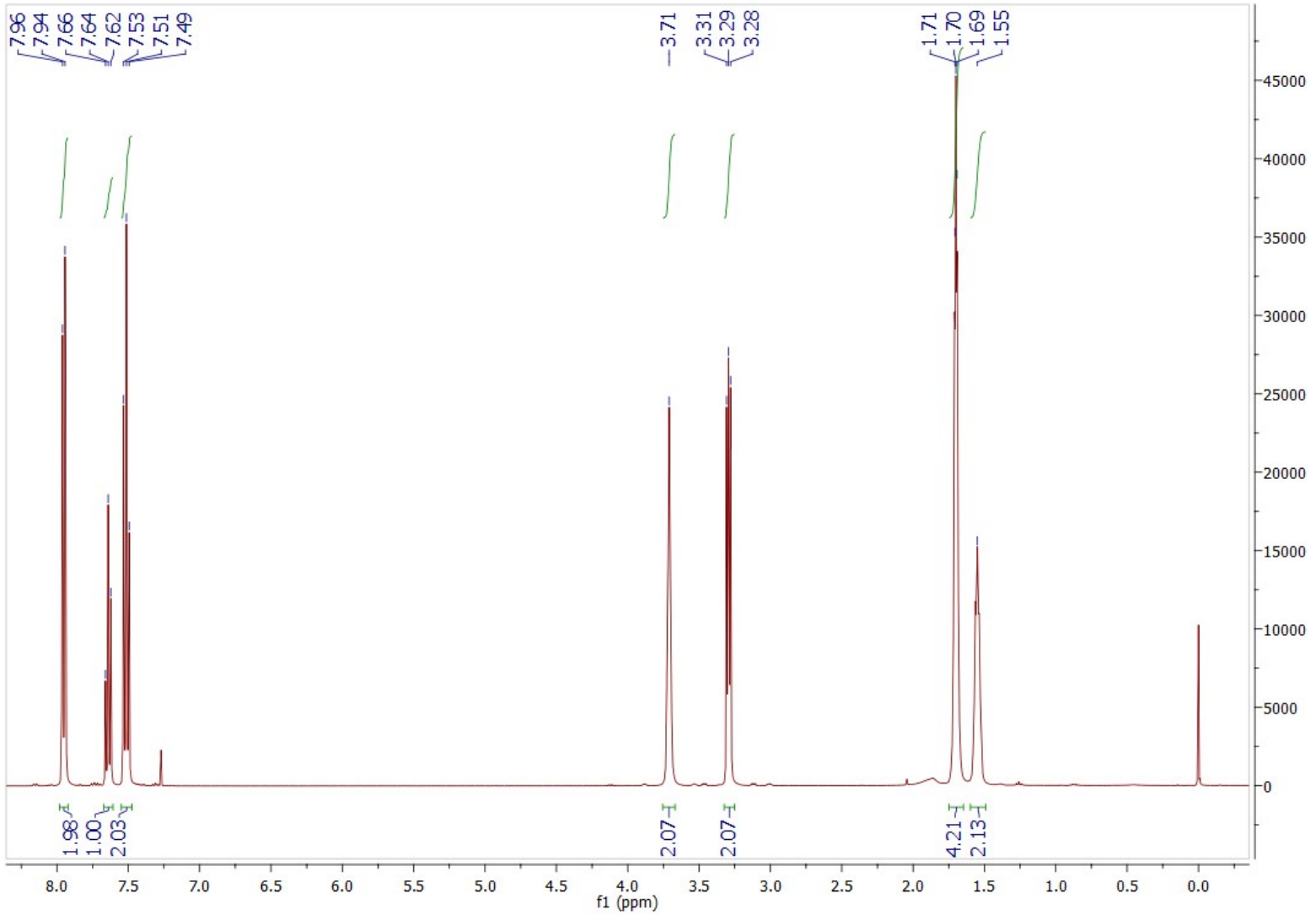

Figure S32. ^{1}H NMR spectrum (400 MHz) of 1-phenyl-2-(piperidin-1-yl)ethane-1,2-dione in $CDCl_3$

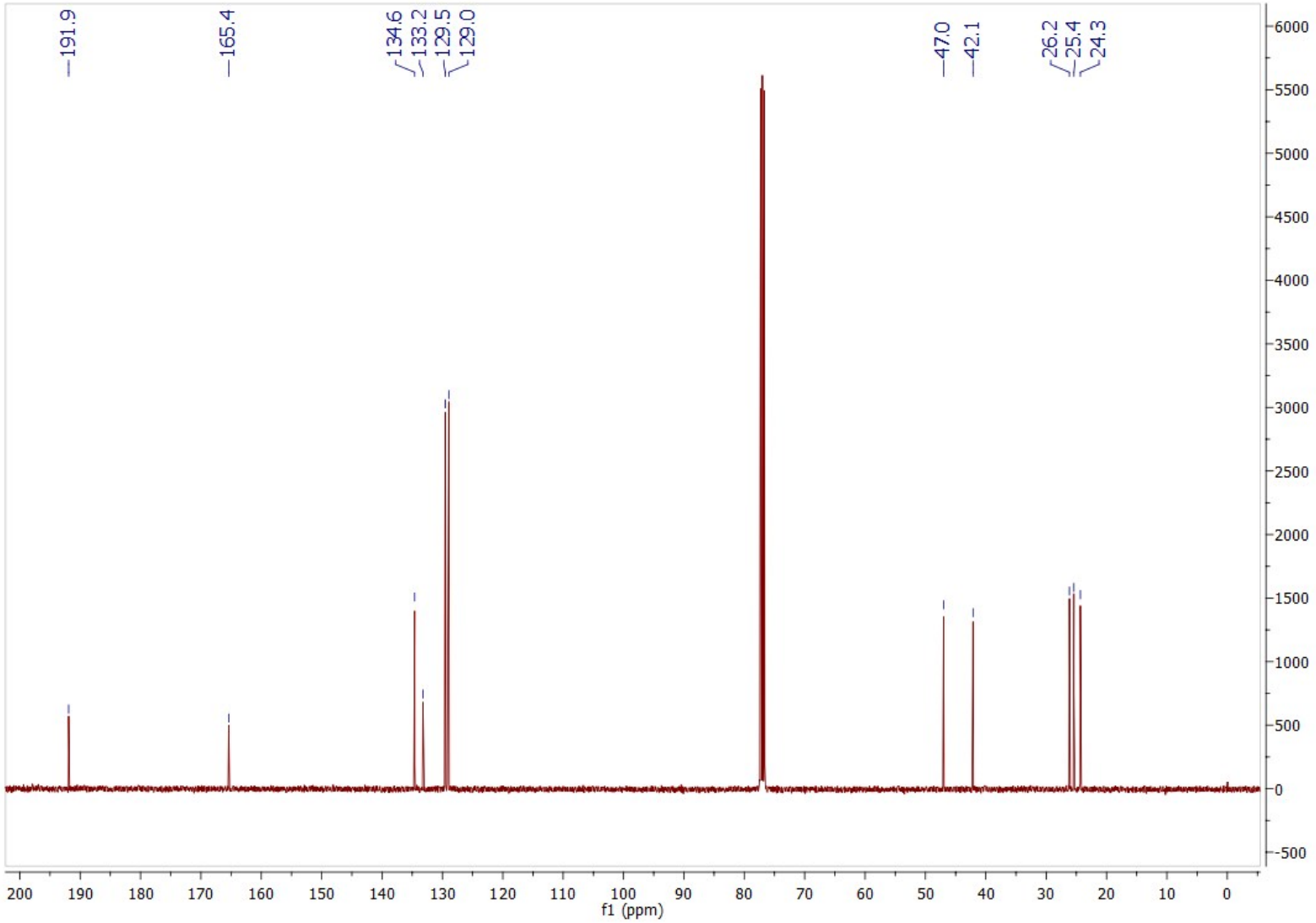

Figure S33. ^{13}C NMR spectrum (100.6 MHz) of 1-phenyl-2-(piperidin-1-yl)ethane-1,2-dione in $CDCl_3$

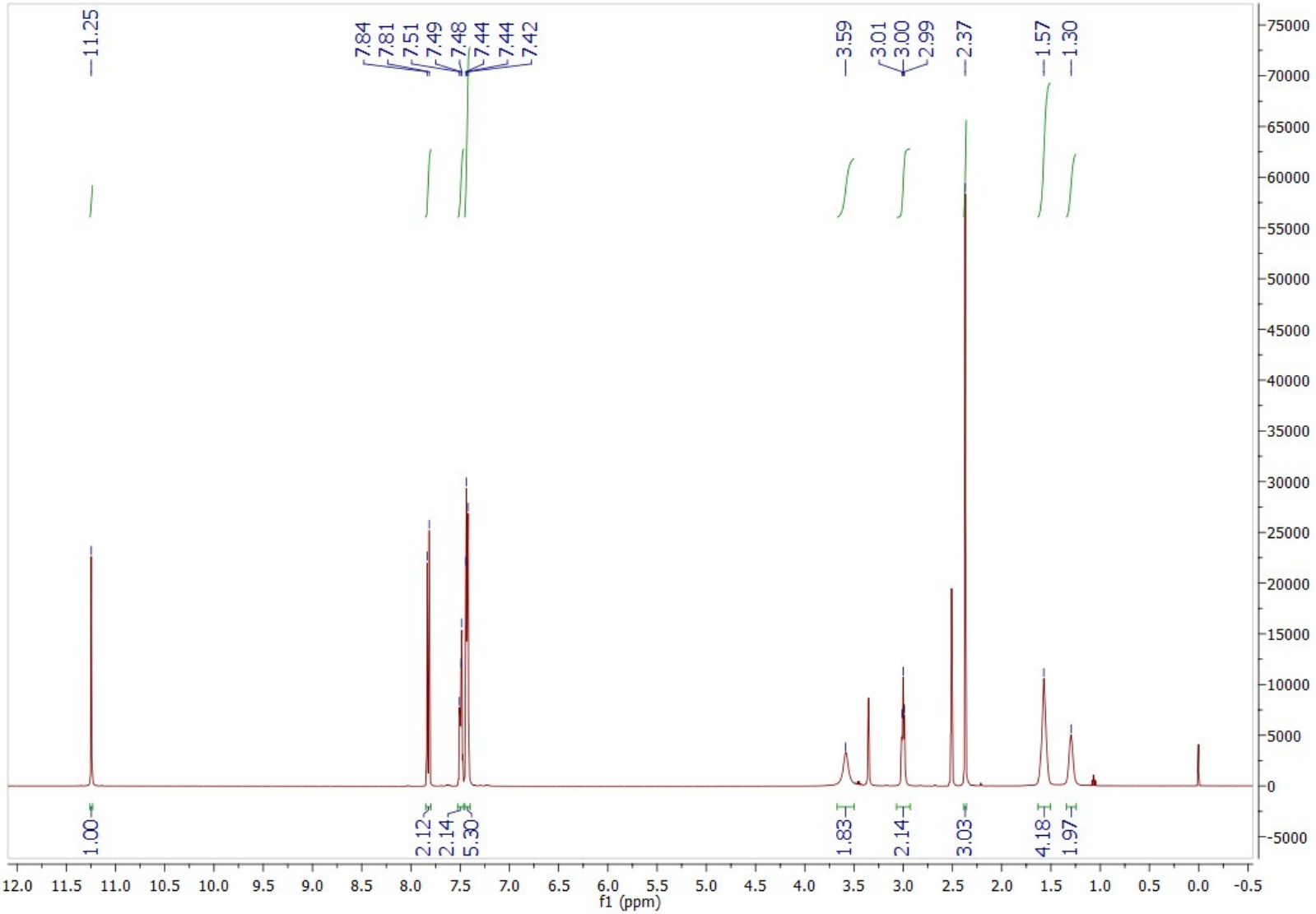

Figure S34. ^{1}H NMR spectrum (400 MHz) of 4-methyl-N'-(2-oxo-1-phenyl-2-(piperidin-1-yl)ethylidene)benzenesulfonohydrazide (**3b**) in DMSO-d_6

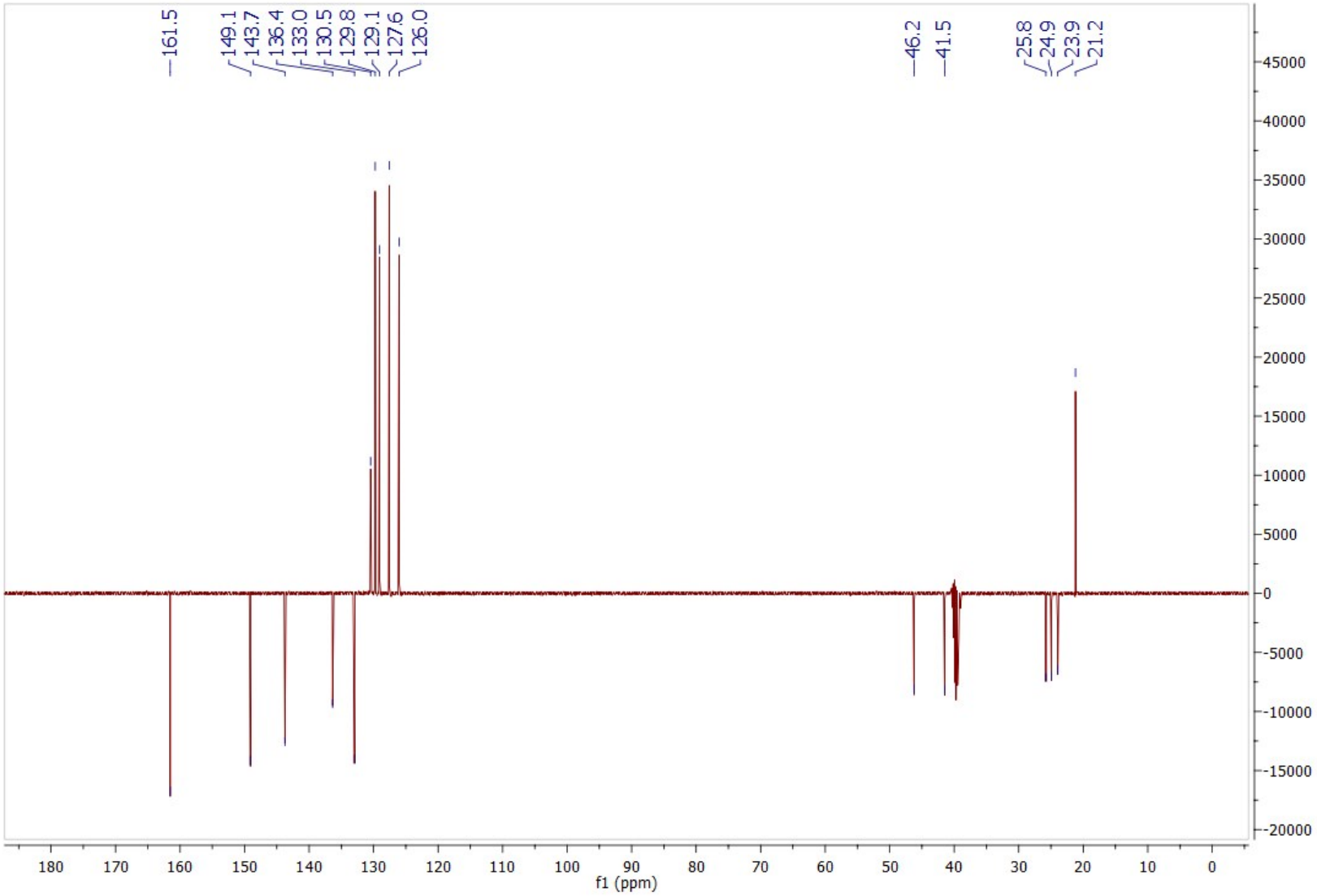

Figure S35. ^{13}C APT NMR spectrum (100.6 MHz) of 4-methyl-N'-(2-oxo-1-phenyl-2-(piperidin-1-yl)ethylidene)benzenesulfonohydrazide (**3b**) in DMSO-d_6

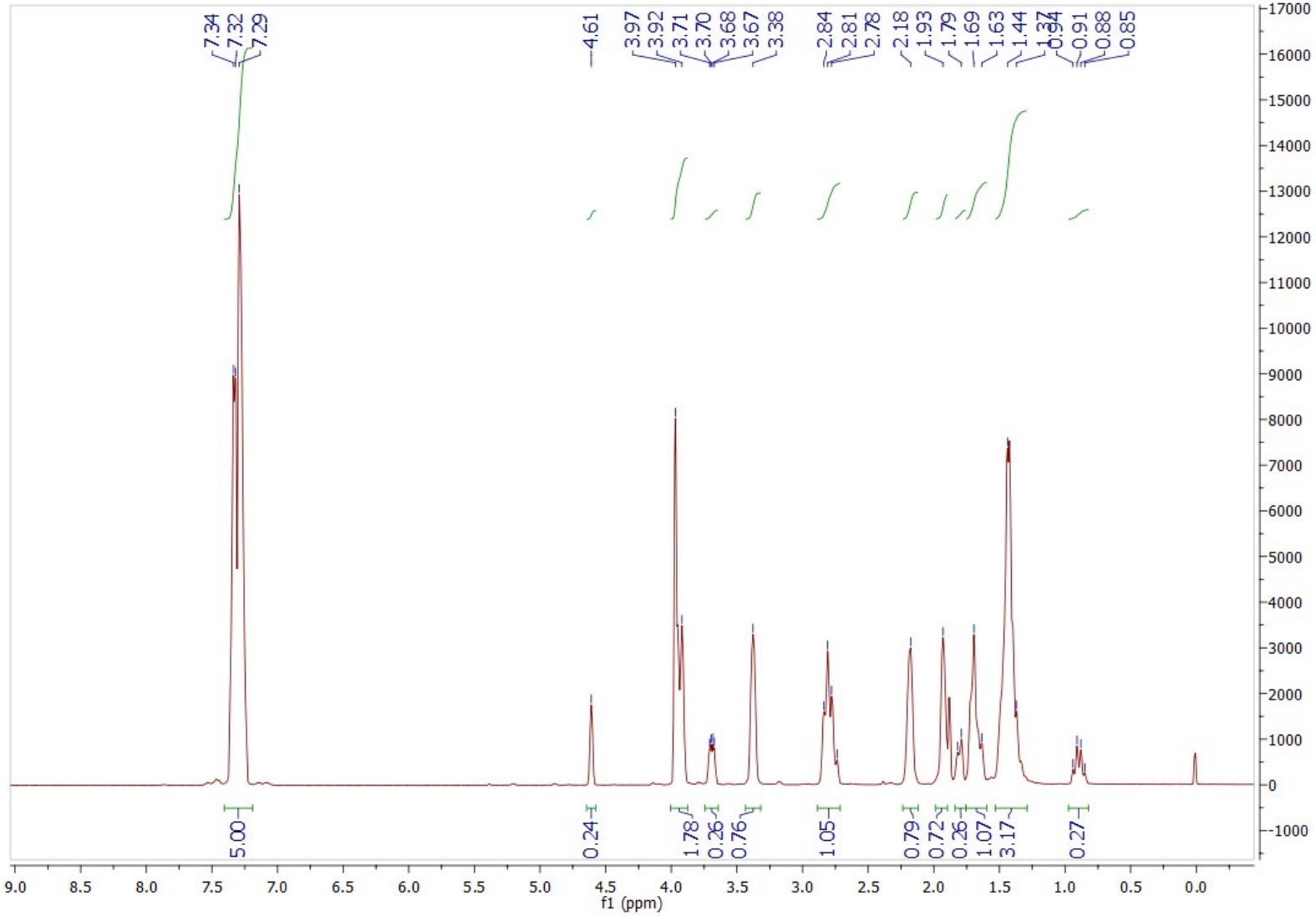

Figure S36. ^{1}H NMR spectrum (400 MHz) of 7-phenyl-1-aza-bicyclo[4.2.0]octan-8-one (**5b**, 3:1 mixture of *threo* and *erythro* isomers) in $CDCl_3$

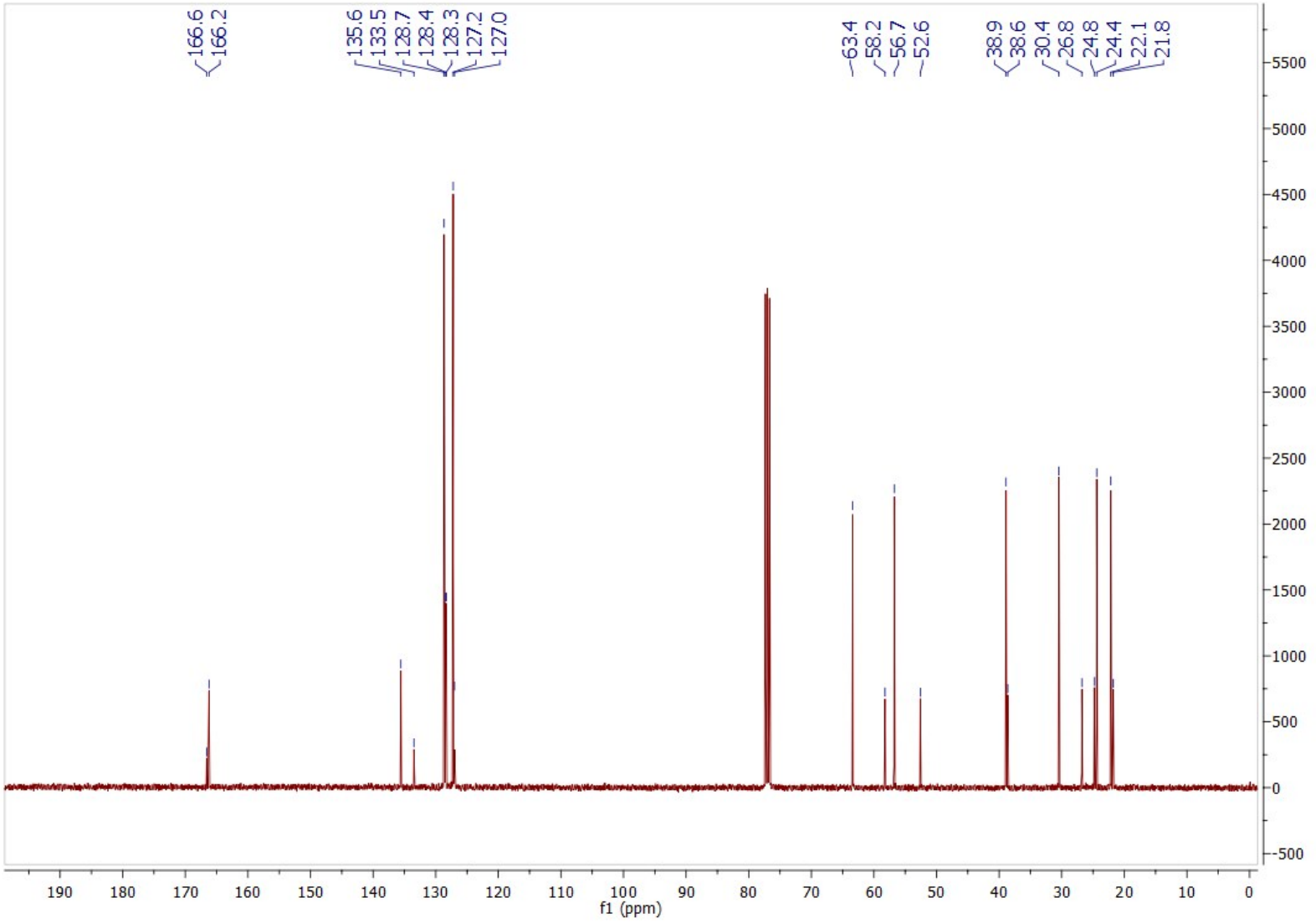

Figure S37. ^{13}C NMR spectrum (100.6 MHz) of 7-phenyl-1-aza-bicyclo[4.2.0]octan-8-one (**5b**, 3:1 mixture of *threo* and *erythro* isomers) in $CDCl_3$

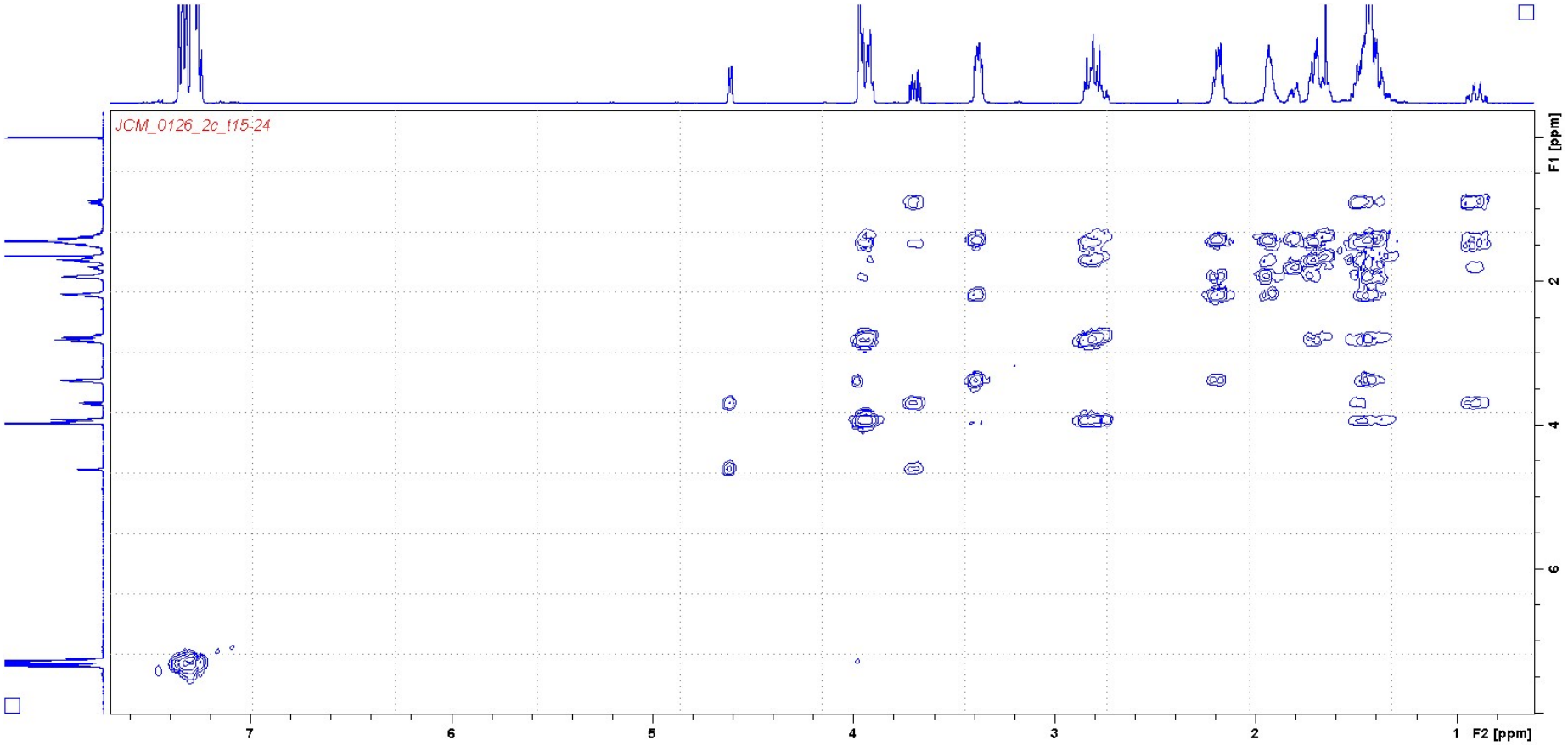

Figure S38. COSY spectrum of 7-phenyl-1-aza-bicyclo[4.2.0]octan-8-one (**5b**, 3:1 mixture of *threo* and *erythro* isomers) in $CDCl_3$

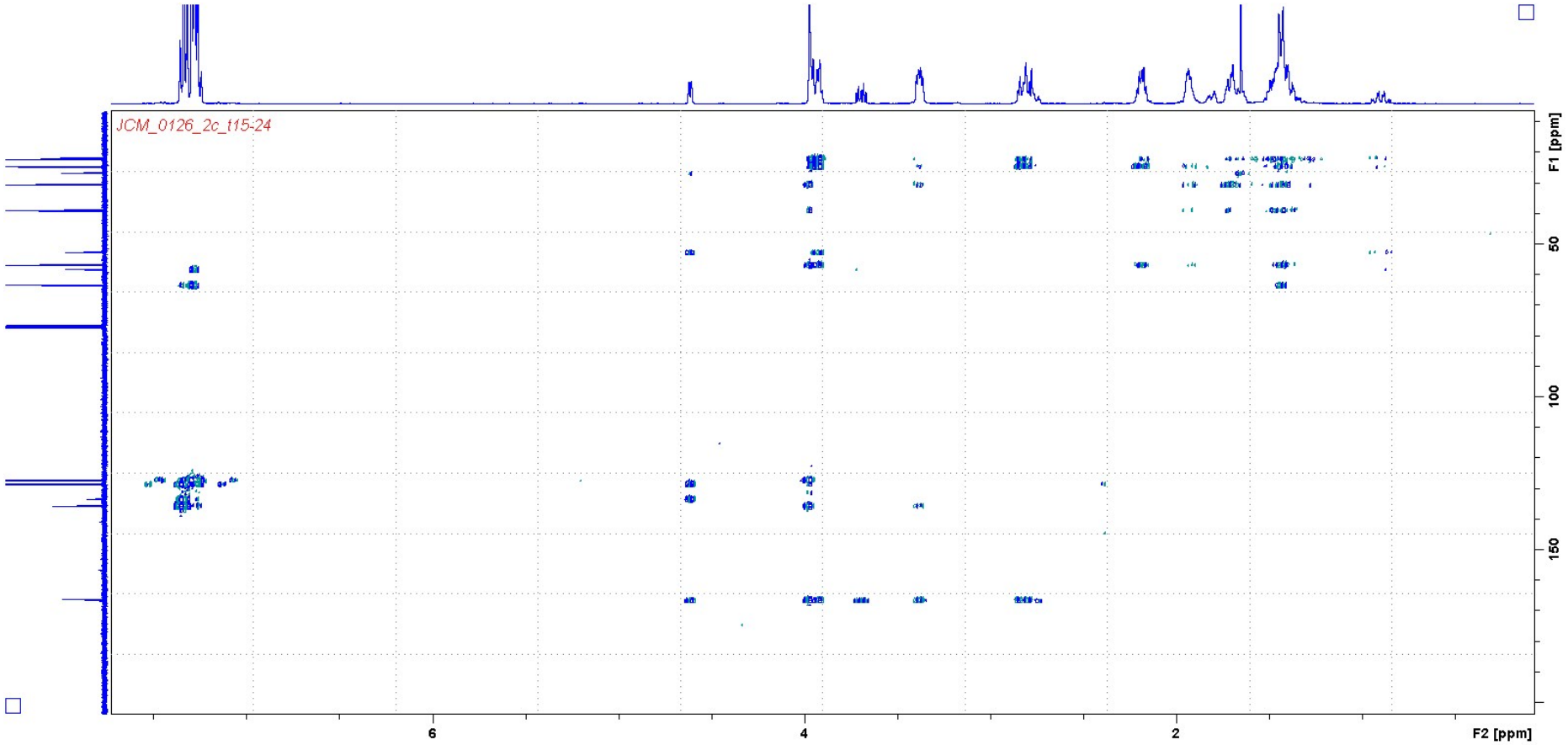

Figure S39. HMBC spectrum of 7-phenyl-1-aza-bicyclo[4.2.0]octan-8-one (**5b**, 3:1 mixture of *threo* and *erythro* isomers) in $CDCl_3$

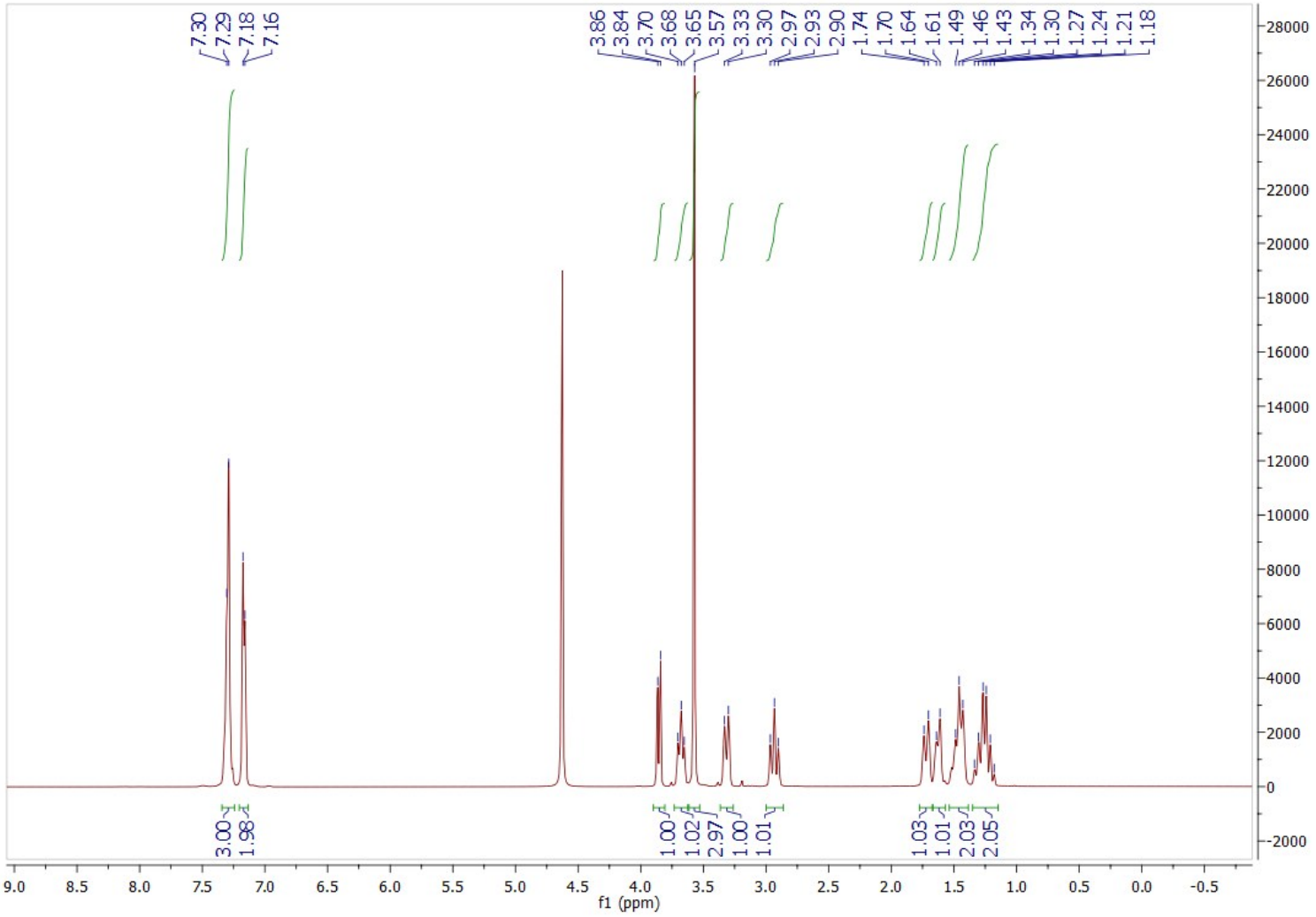

Figure S40. ^{1}H NMR spectrum (400 MHz) of *threo*-methylphenidate (**1a** + **1b**) hydrochloride in D_2O

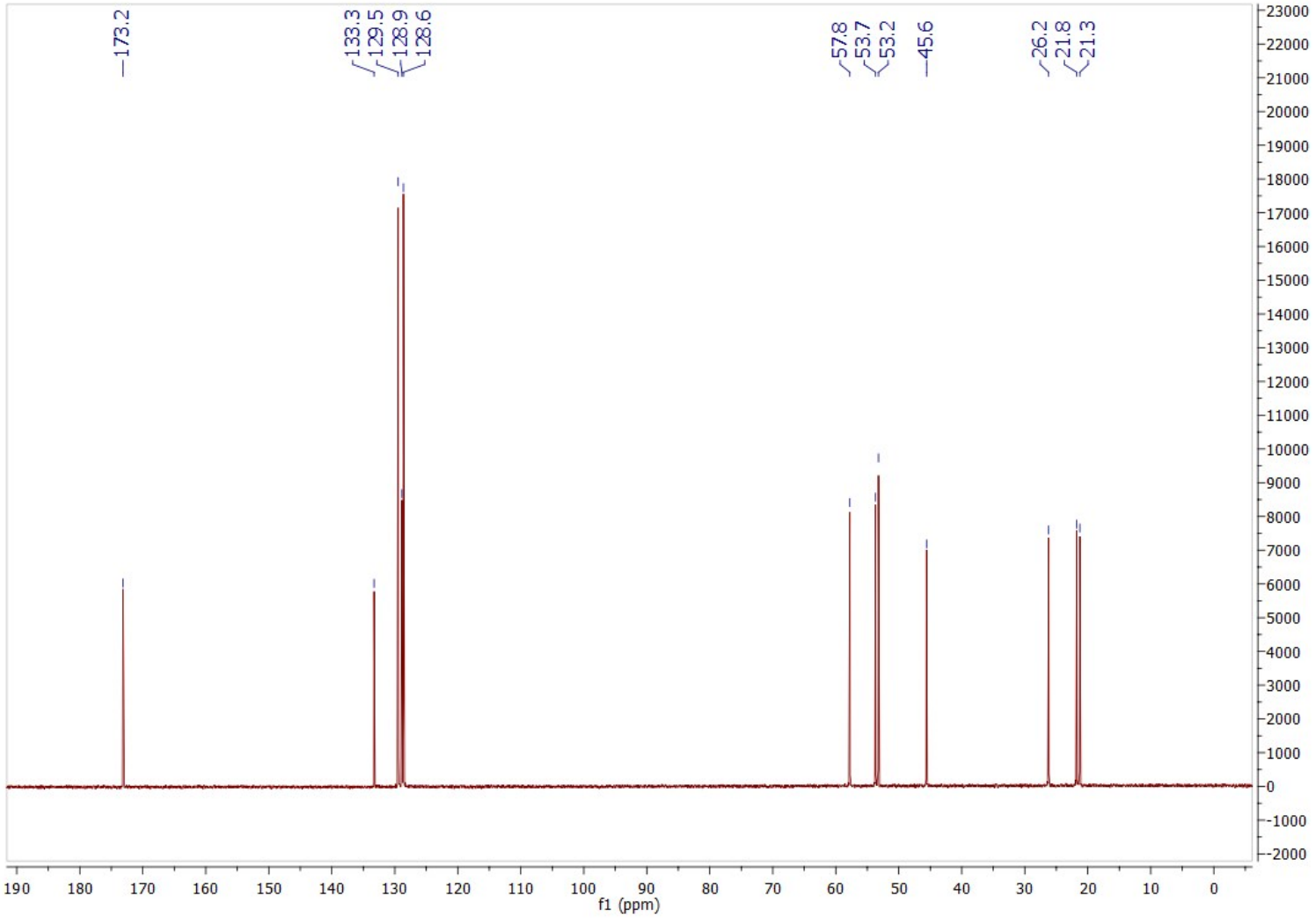

Figure S41. ^{13}C NMR spectrum (100.6 MHz) of *threo*-methylphenidate (**1a** + **1b**) hydrochloride in D_2O

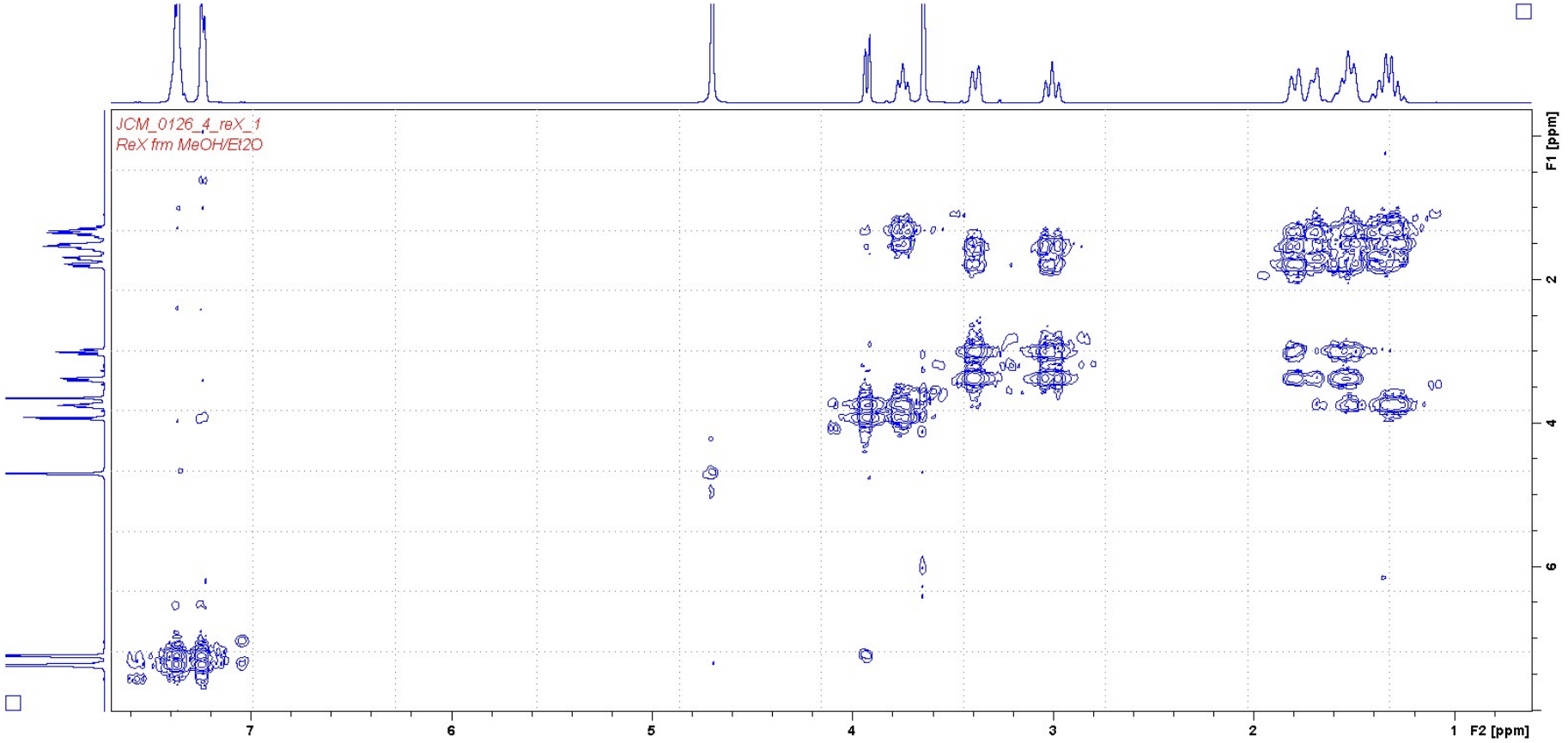

Figure S42. COSY spectrum of *threo*-methylphenidate (**1a** + **1b**) hydrochloride in D_2O

2.6 Copies of GC and HPLC chromatograms

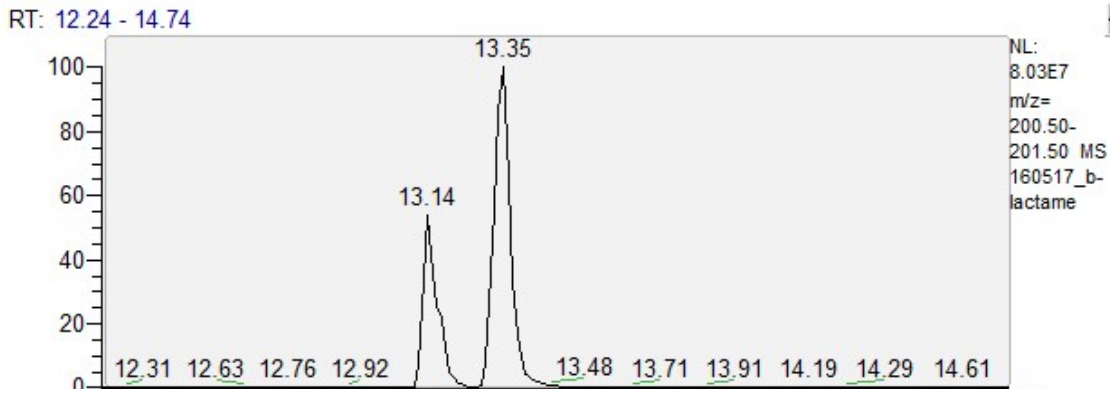

Figure S43. Gas chromatography on β-lactam **5b** (3:1 *threo/erythro*)

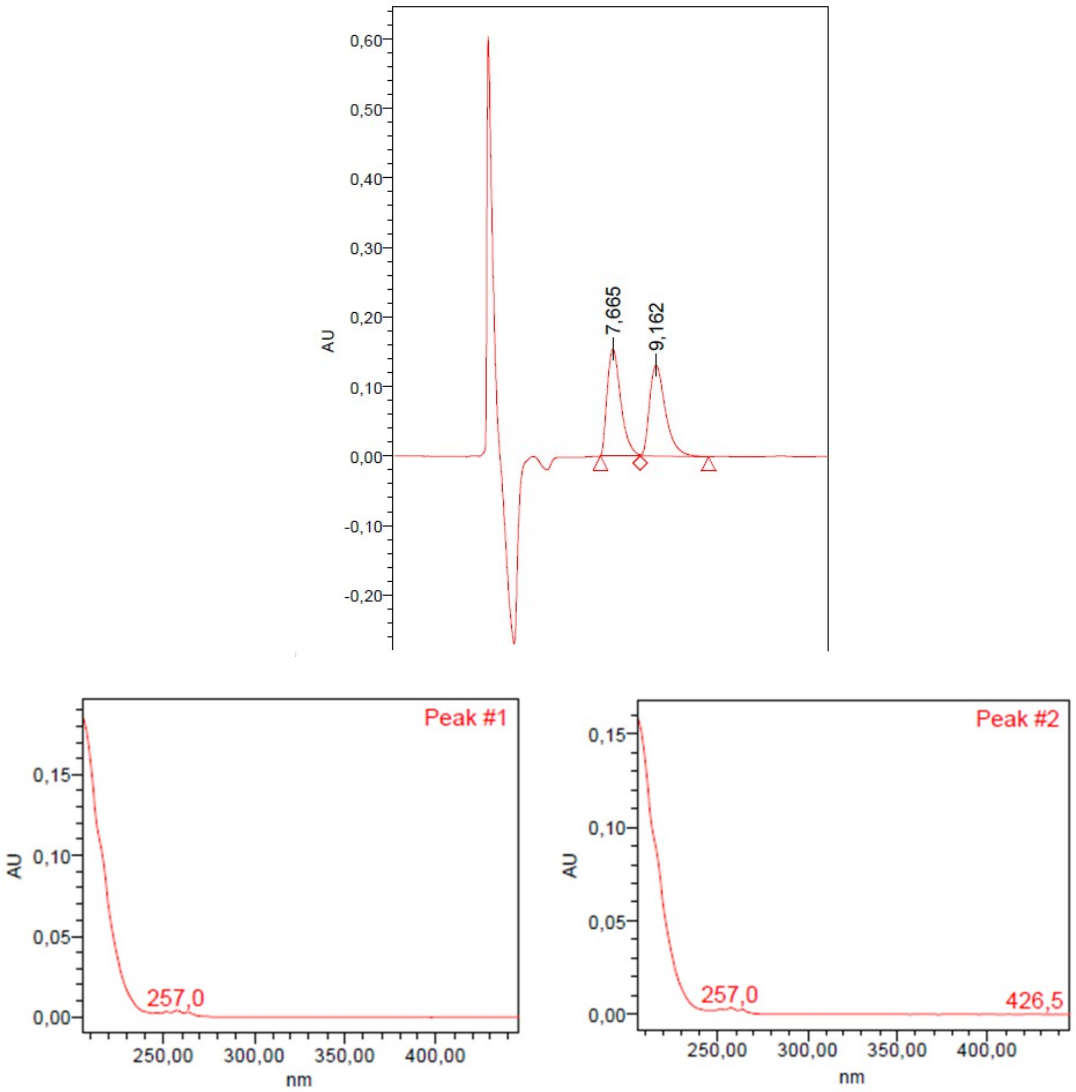

Figure S44. Chiral HPLC chromatogram and the corresponding UV spectra resulting from the analysis on recrystallized *threo*-**1**·HCl racemate showing the (2*R*,2'*R*)-*threo* **1a** and (2*S*,2'*S*)-*threo* **1b** enantiomers

3 References

S1 R. W. Bates, R. Iah N. Khanizeman, H. Hirao, Y. S. Tay and P. Sae-Lao, *Org. Biomol. Chem.*, 2014, **12**, 4879–4884.

S2 D. G. Brown, E. J. Velthuisen, J. R. Commerford, R. G. Brisbois and T. R. Hoye, *J. Org. Chem.*, 1996, **61**, 2540–2541.

S3 X. Hu, J. Sun, H.-G. Wang and R. Manetsch, *J. Am. Chem. Soc.*, 2008, **130**, 13820–13821.

S4 R. Katritzky, M. El Khatib, O. Bol'shakov, L. Khelashvili and P. J. Steel, *J. Org. Chem.*, 2010, **75**, 6532–6539.

S5 J. V. Ruppel, J. E. Jones, C. A. Huff, R. M. Kamble, Y. Chen and X. P. Zhang, *Org. Lett.*, 2008, **10**, 1995–1998.

S6 D. T. Whitaker, K. S. Whitaker and C. R. Johnson, *Encyclopedia of Reagents for Organic Synthesis*, John Wiley & Sons, Ltd, Chichester, 2001.

S7 D. Mehetre, S. Ghadge, A. Chabukswar and P. Lokhande, *Int. J. Pharm. Phytopharm. Res.*, 2013, **2**, 412–414.

S8 W. R. R. Harker, E. L. Carswell and D. R. Carbery, *Org. Lett.*, 2010, **12**, 3712–3715.

S9 N. Takasu, K. Oisaki and M. Kanai, *Org. Lett.*, 2013, **15**, 1918–1921.

S10 S. Chiba, L. Zhang, S. Sanjaya and G. Y. Ang, *Tetrahedron*, 2010, **66**, 5692–5700.

S11 J. M. Axten, L. Krim, H. F. Kung and J. D. Winkler, *J. Org. Chem.*, 1998, **63**, 9628–9629.

S12 D. Shanmugapriya, R. Shankar, G. Satyanarayana, V. H. Dahanukar, U. K. Syam Kumar and N. Vembu, *Synlett*, 2008, 2945–2950.

S13 M. Hu, J. Rong, W. Miao, C. Ni, Y. Han and J. Hu, *Org. Lett.*, 2014, **16**, 2030–2033.

S14 J. M. Axten, R. Ivy, L. Krim and J. D. Winkler, *J. Am. Chem. Soc.*, 1999, **121**, 6511–6512.

S15 B. Grzeszczyk, K. Poławska, Y. M. Shaker, S. Stecko, A. Mames, M. Woźnica, M. Chmielewski and B. Furman, *Tetrahedron*, 2012, **68**, 10633–10639.

S16 H. M. L. Davies, T. Hansen, D. W. Hopper and S. A. Panaro, *J. Am. Chem. Soc.*, 1999, **121**, 6509–6510.

S17 D. L. Thai, M. T. Sapko, C. T. Reiter, D. E. Bierer and J. M. Perel, *J. Med. Chem.*, 1998, **41**, 591–601.